Regional scale hydrodynamic modeling of the river-floodplain-reservoir continuum

A. S. Fleischmann[1]*, J. P. F. Brêda[1], O. A. Passaia[12], S. C. Wongchuig[13], F. M. Fan[1], R. C. D. Paiva[1], G. F. Marques[1], W. Collischonn[1]

[1]Instituto de Pesquisas Hidráulicas (IPH), Universidade Federal do Rio Grande do Sul (UFRGS), Porto Alegre, Brazil, Av. Bento Gonçalves, 9500, ZIP-code: 91501-790.

[2]Fundação Cearense de Meteorologia e Recursos Hídricos (FUNCEME), Fortaleza, Brazil, Av. Rui Barbosa, 1246, ZIP-code: 60115-221.

[3]Univ. Grenoble Alpes, IRD, CNRS, Grenoble INP, Insitut des Géosciences de l'Environnement (IGE, UMR 5001), 38000, Grenoble, France

*Corresponding author: Ayan Santos Fleischmann (ayan.fleischmann@gmail.com)

Keywords: Hydrological Modeling, Large Scale Modeling, Hydropower, Flood Dynamics, Paraná River Basin, MGB

Abstract

River floodplains and reservoirs interact throughout a basin drainage network, defining a coupled human-water system with multiple feedbacks. Recent modeling developments have aimed to improve the representation of such processes at regional to continental scales. However, most large-scale hydrological models adopt simplified lumped reservoir schemes, where an offline routine is run with inflows estimated by the model, with limited consideration of the complementarity between floodplains and reservoirs on attenuating floods at regional scale. This paper presents a novel approach that fully couples river-floodplain-reservoir hydrodynamic and hydrological models, significantly improving the representation of reservoir dynamics and operation in the river-floodplain-reservoir continuum at large scale and across multiple dam cascades. The model is applied to the Paraná River Basin with explicit simulation of 31 large dams and river hydraulic variables at basin scale. Three types of reservoir bathymetry representation are compared, from lumped to distributed methods, combined with three reservoir operation schemes and varying degrees of input data requirement within two parameterization scenarios (global and regional setups). The operation schemes were more relevant than the reservoir bathymetry representation to estimate downstream flows and water levels. While the data-driven operation scheme, based on linear regressions between observed water levels and dam outflows, provided the best estimates of both active storage and discharges, the more generic operation reasonably estimated discharges and peak attenuation, albeit not as accurately for active storage. The global parameterization of reservoir operation resulted in poorer performance compared to the regional-based one, but it satisfactorily modeled discharge and peak attenuation. Regarding the reservoir bathymetry representation, a basin scale comparison of the lumped and distributed schemes indicated the inability of the former

to represent backwater effects. This was further corroborated by validating the longitudinal water level profile of Itaipu dam with ICESat satellite altimetry data. Finally, the model was used to show the complementarity between floodplains and reservoirs on attenuating floods at regional scale. Large scale models should move beyond offline coupling strategies, and include regional-based, data-driven reservoir operation schemes together with a distributed representation of reservoir bathymetry into river-floodplain hydraulic schemes. This will largely improve the estimation of river discharges, water levels and flood storage, and thus the model ability to represent the regional scale river-floodplain-reservoir continuum.

1 Introduction

Reservoirs are important infrastructure for energy production, flood control, flow regulation and water supply, among other uses (Lehner et al., 2011). Their construction and operation have also led to major socio-environmental concerns (Grill et al., 2019; Nilsson, 2005; Poff et al., 2010; Richter and Thomas, 2007), and efforts to improve storage allocation (Almeida et al., 2019; Ho et al., 2017; Schmitt et al., 2019). Reservoirs, however, operate in basins with a continuum in the river system connecting it to rivers and floodplains, through which human societies and ecosystems interact with dynamic two-way feedbacks (Di Baldassarre et al., 2013; Pande and Sivapalan, 2017; Viglione et al., 2014). At regional to continental scales, this river-floodplain-reservoir continuum is associated to a complex relationship among surface water processes. For example, in the La Plata River Basin in South America, dozens of large reservoirs have been built since the 1950's interacting with complex wetland systems as the Pantanal,

Esteros del Iberá and Paraná floodplains (Minotti, 2018). In the basin, human society has settled around floodplains for centuries, leading to a fully coupled human-water system (Doyle and Barros, 2011; Lee et al., 2018). As the use and development of the floodplain by society evolve, there is an increasing need to better understand the hydrodynamic interactions in this river-floodplain-reservoir continuum, so we can better design and operate water systems to cope with human and ecosystem demands considering hydrological uncertainty, processes and current and future environmental changes.

Regional to continental scale hydrological-hydrodynamic models provide a unique opportunity to address these needs. While recent advances in large scale modeling have improved our capability to simulate river floods at both 1D and 2D dimensions (Bates et al., 2018; Fleischmann et al., 2020; Neal et al., 2012; Paiva et al., 2013; Schumann et al., 2013; Trigg et al., 2016; Yamazaki et al., 2011), most studies on reservoir simulation have focused on representing dam storage and operation (i.e., a water management model) within simpler hydrological models, with less physically based flow routing methods (Droppers et al., 2020; Hanasaki et al., 2018; Yassin et al., 2019). In the studies by Mateo et al. (2014) and Pokhrel et al. (2018), for instance, a hydrodynamic model was run (offline) with observed or simulated dam outflows at the grid cell related to the dam, in order to estimate alterations in downstream flooding. Difficulties for detailed reservoir simulation included the unknown bathymetry and specific dam operation at very large scales, and are also a challenge.

Only recently the hydrodynamics of dam cascades were explicitly included into regional hydrodynamic models (Shin et al., 2019; Fleischmann et al., 2019a), aiming at representing the river-floodplain-reservoir system with a fully-coupled approach that allowed a distributed representation of variables as discharges, water levels and flood

extent and storage in human-altered systems. As the representation of these processes improves, a better and integrated assessment of basin water resources and floods becomes possible. Examples include the understanding of the relative role of floodplains and reservoirs on flood attenuation (Fleischmann et al., 2019a), more detailed simulation of evaporation (Shin et al., 2019), and understanding of the reservoir influence on local climate (Degu et al., 2011; Hossain et al., 2012). The representation of the reservoir dynamics itself and associated backwater effects and flooding in upstream areas, and simulation of carbon cycle and phytoplankton dynamics (e.g., lake emissions and degassing or downstream emissions; Bierkens et al. (2015)), can also benefit from such modeling systems. Ultimately, these tools will provide an important basis towards a fully coupled and distributed human-water modeling system within hyperresolution Earth system models (Nazemi & Wheater, 2015; Pokhrel et al., 2016; Wood et al., 2011), adopting detailed grids and daily temporal resolution (Gutenson et al., 2020; Zajac et al., 2017).

Regarding the representation of dam operation in regional to global models, there have been major improvements since pioneering studies by Hanasaki et al. (2006) and Haddeland et al. (2006), which have been used and adapted for many studies (Adam et al., 2007; van Beek et al., 2011; Biemans et al., 2011; Pokhrel et al., 2012; Shin et al., 2019; Wisser et al., 2010). Since these first generic algorithms, data-driven reservoir operation schemes are now feasible, while optimization methods have also been developed, involving storage, outflow and inflow observations (Solander et al., 2016; Wu and Chen, 2012; Yassin et al., 2019), and downstream water or energy demands (Haddeland et al., 2006). All these developments highlight the ongoing necessity to better estimate actual reservoir operation in order to achieve hyperresolution models that are locally relevant. Cross-scale comparisons among different approaches, from

simpler, globally-based, to more complex, regionally-derived setups, can yield meaningful insights on the ways forward, especially using regionally set up models (Fleischmann et al., 2019c; Nazemi & Wheater, 2015; Trigg et al., 2016).

The need for a fully-coupled approach was explicitly highlighted by some authors (Fleischmann et al., 2019a; Shin et al., 2019). However, the benefits of representing the reservoir dynamics fully coupled within the river-floodplain-reservoir continuum processes with a distributed approach, over the traditional lumped and offline representation, remains a knowledge gap in the field for large scale models. The extent to which simple, level-pool reservoir simulations (i.e., lumped) may lead to similar results as distributed (i.e., dynamic), more complex ones, is not yet understood. Finally, a correct reservoir operation also needs to be incorporated to improve the understanding of the human feedback in the river-floodplain-reservoir continuum.

This study brings a novel contribution to these gaps with an improved representation of the river-floodplain-reservoir interactions within hydrologic-hydrodynamic models, followed by a broad analysis of the continuum of hydraulic variables basin-wide considering the reservoir operation effects. The contributions of this study address three main research questions: (i) what are the differences between simulating lumped and distributed reservoir bathymetry in coarse-scale, online coupled hydrologic-hydrodynamic models, in terms of different variables as water levels, discharge, flood extent and storage, and evapotranspiration? (ii) how do generic and more data-driven reservoir operation schemes differ in terms of hydrological variables estimation in regional scale models? And (iii) what is the relative role of floodplains and reservoirs on flood attenuation in large-scale anthropized systems, considering basin-wide hydrological processes? To answer these questions, new modeling approaches to improve reservoir representation and operation are proposed and tested in

a ~950,000 km² watershed (Upper Paraná River Basin, Brazil). Different simulation scenarios are performed to assess the dynamics of reservoirs in terms of complexity of bathymetry representation (lumped to distributed) and reservoir operation (from generic to data-driven approaches, and from globally to regionally derived parameterizations).

2 Methods

2.1 Study area: The Upper Paraná River Basin

The Upper Paraná River Basin (**Figure 1**) was selected as a study area given (i) its large number of dam cascades (in parallel and in series); (ii) the existence of large floodplains both upstream and downstream of dam cascades; and (iii) the availability of observed daily time series of dam inflows, outflows and storage from the Brazilian National Water Agency (ANA). Those are desirable characteristics to address in large scale modeling of river-floodplain-reservoir systems.

The Paraná River is formed by the confluence of Grande and Paranaíba rivers in Brazil, with major tributaries being the Tietê, Paranapanema, Ivaí and Iguaçu rivers, all in its left margin. The Upper Paraná River Basin has a drainage area of ~950,000 km² and it is among those with the largest hydropower installed capacity in the world (and almost 50% of the installed hydropower capacity of Brazil), including the Itaipu dam (ID 18 in **Figure 1**) which is one of the largest dams in the world (Itaipu, 2018). Large cities as São Paulo and Brasília (Brazil Federal Capital) are located within the basin, which holds a population of nearly 70 million people. The wet period usually occurs from November/January to May/June (Agostinho et al., 2000), with average annual

rainfall of about 1400 mm (Boulanger et al., 2005)**.** There are contrasting hydroclimatic regions throughout the basin, with the northern (southern) regions presenting a seasonal (non-seasonal) precipitation regime.

The basin has 86 large dams (> 30 MW) in operation, with an installed capacity of 48,083 MW (ANEEL, 2020) (**Figure 1**). There are also 500 (58) small (large) proposed, planned or under construction dams, related to 5,643 (3,909) MW of installed capacity, respectively (ANEEL, 2020). Sixty-two large dams are currently connected to the Brazilian National Interconnected System (SIN), with 32 run-of-river and 30 flow regulation dams (ONS, 2020), which are coordinately operated with other power sources (e.g., thermal and wind) to generate and distribute energy to the whole system minimizing costs (Marques & Tilmant, 2013). Most dams are also operated with multiple uses, such as flood control, water supply and navigation. Overall, there is a large hydrological alteration at the basin scale due to reservoir operation (Santos, 2015). The extensive floodplains throughout the basin, as the 230 km reach in the Paraná mainstem between Porto Primavera and Itaipu dams, harbor important ecosystem services (Agostinho et al., 2001, 2008; Baumgartner et al., 2018).

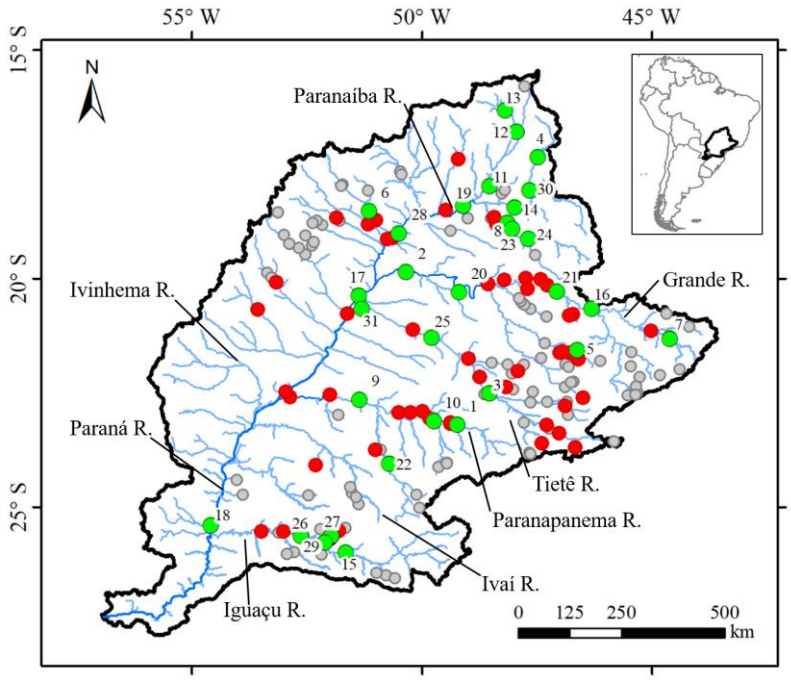

Figure 1. The Upper Paraná River Basin within South America, and the 31 simulated (green circles) and other non-simulated Brazilian dams (red: large dams – installed capacity > 30 MW; grey: small dams – capacity between 3 and 30 MW). The total number of large dams is 86 (green and red dots). Rivers of interest are labeled.

2.2 Hydrological and hydrodynamic representation of the river-floodplain-reservoir continuum

The MGB model ("Modelo de Grandes Bacias" in Portuguese, an acronym meaning "Model of Large Basins") (Collischonn et al., 2007; Pontes et al., 2017) is used to implement and test the proposed representation of the river-floodplain-reservoir continuum and reservoir operation. It is a semi-distributed, hydrological-hydrodynamic model developed to simulate large-scale basins. This model is chosen given its proven track record of simulation in several other river basins at different scales, from regional to continental domains (Siqueira et al., 2018). First, the original MGB modeling

approach is presented, followed by the proposed improved representation of the reservoirs and their hydraulic and hydrodynamic relationships with the continuum.

In MGB's representation, the basin is divided into unit-catchments of equal river lengths, and within each the model simulates vertical hydrological processes as evapotranspiration, soil water infiltration and runoff generation (from surface, subsurface and groundwater reservoirs) (**Figure 2**). Local runoff is added as a lateral boundary condition to the drainage network, and a hydrodynamic routing is performed to simulate river, floodplains and reservoirs' surface water dynamics. Soil and vegetation model parameters are defined for each Hydrologic Response Units (HRU's) within a given sub-basin, and the HRU's are derived from a combination of soil and vegetation maps. Evapotranspiration is computed with the Penman-Monteith equation for soil/vegetated areas, and Penman equation for flooded areas (i.e., assumed as open water). A dynamic two-way feedback between the hydrologic and hydrodynamic modules is also considered, by which floodplain water can infiltrate into the unsaturated soil, and evapotranspiration/open water evaporation and runoff generation are dynamically computed considering the surface flooded fraction at each time step. More details on the hydrological model are presented in Supplementary Material S2 and in Collischonn et al. (2007), Pontes et al. (2017) and Siqueira et al. (2018). Recent MGB applications in the Paraná basin with the simpler, Muskingum-Cunge flood routing scheme were performed in Fleischmann et al., (2019b) and Quedi & Fan, (2020).

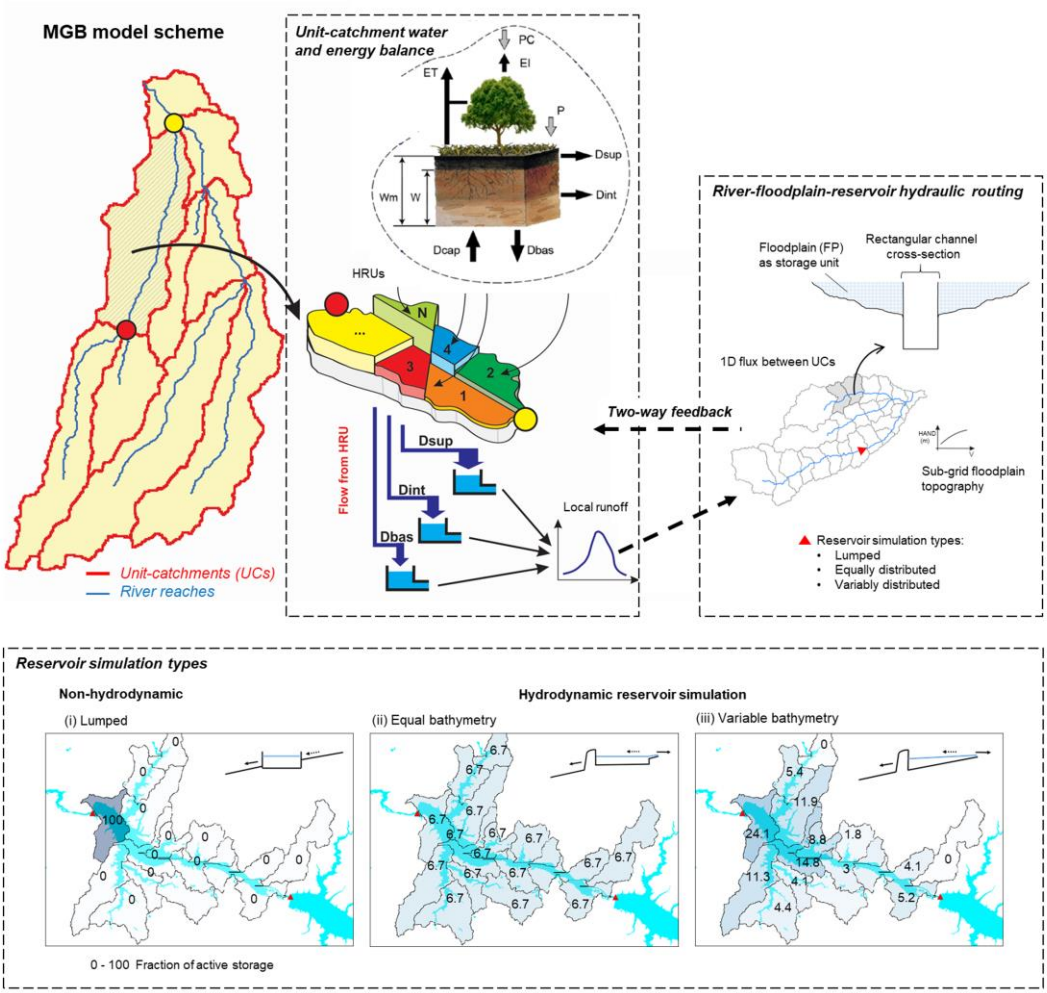

223

224 **Figure 2**. Overview of the MGB model structure: unit-catchment water and energy balance
225 (middle panel), river-floodplain-reservoir hydraulic routing (upper right), and types of reservoir
226 simulation (bottom panel).

227

228 2.2.1 MGB model river-floodplain hydrodynamic routing

229

230 The local inertia explicit method proposed by Bates et al. (2010) is adopted
231 within MGB to simulate 1D flow propagation along the drainage network. This method
232 is a simplification of Saint-Venant equations, neglecting the convective acceleration
233 term from the momentum equation, which has been proven satisfactory to represent

234 flood wave transport along rivers at both 1D and 2D dimensions (Getirana et al., 2017;
235 Neal et al., 2012; Siqueira et al., 2018; Yamazaki et al., 2013). Within MGB,
236 floodplains are represented as storage units, i.e., they are ineffective areas without active
237 flow, river-floodplain water exchange is instantaneous, and water surface elevation is
238 assumed the same along the river-floodplain system within a given unit-catchment
239 (Paiva et al., 2011). Channel cross sections are assumed rectangular, as typically
240 adopted in large scale hydraulic modeling (Paiva et al., 2013; Trigg et al., 2009).

241 The flux between two adjacent unit-catchments is computed with the discretized
242 momentum Equation 1:

243 $$Q_{out,i}^{t+\Delta t} = \frac{Q_i^t - gB_i\Delta t h_i S_i}{1+\frac{g\Delta t|Q_i^t|n^2}{B_i(h_i)^{7/3}}}$$ Equation 1

244 Where $Q_{out,i}^{t+\Delta t}$ is the discharge at unit-catchment i at time $t+\Delta t$, n is the Manning's
245 coefficient, h_i the flow depth between unit-catchments i and $i+1$, S_i the water surface
246 level slope, Δt the model time step, B_i the flow width, and g the gravitational
247 acceleration.

248 The continuity equation can be approximated for each unit-catchment river reach
249 as:

250 $$\frac{V_i^{t+\Delta t} - V_i^t}{\Delta t} = \sum Q_{in,i}^{t+\Delta t} - Q_{out,i}^{t+\Delta t} + Q_{local} + P_i - E_i$$ Equation 2

251 Where V is the stored volume in unit-catchment i, $\sum Q_{in,i}^{t+\Delta t}$ the sum of inflows from
252 upstream unit-catchments, Q_{local} the locally generated runoff, P the precipitation over
253 flooded areas (i.e. river reach surface area plus flooded floodplain or reservoir area), and
254 E the flooded area open water evaporation computed with Penman equation.

Once the unit-catchment volume is updated with (2), water level in the unit-catchment is estimated from its level-volume relationship (hypsometric curve). For stages below bank elevation, this is derived from the channel cross section. For stages above bank elevation, it represents the floodplain topography, and it is obtained with a GIS pre-processing step that computes flooded areas associated to increments in Height Above Nearest Drainage values (HAND; Rennó et al. (2008)) extracted from the SRTM Digital Elevation Model (DEM) (Siqueira et al., 2018).

Effective hydraulic parameters that are required for each river reach are channel bed elevation, cross section bankfull width and depth, and Manning roughness coefficient. Bed elevation is derived for each unit-catchment from the average DEM river network pixels (Siqueira et al., 2018) subtracted by bankfull depth. The hydrodynamic routing time step is determined by the Courant-Friedrichs-Levy condition with an additional multiplier parameter for ensuring model numerical stability (Bates et al., 2010; Yamazaki et al., 2011).

2.3 Reservoir routing

Two main aspects differ the proposed improved reservoir representation from the original MGB river-floodplain routing scheme. First, at the unit-catchment corresponding to the dam location, the momentum equation (1) is replaced by the dam outflow equation (i.e., it is set as an internal boundary condition), which is based on simple spillway or outlet works equations, or on more complex reservoir operation derived from actual dam operational data.

Second, the reservoir storage (and bathymetry) is represented in MGB by adjusting the level-volume relationship in the unit-catchments located within the reservoir lake, originally extracted from a DEM. If the dam did not exist during the DEM acquisition date, the storage is already represented in the level-volume relationships, and thus no correction is necessary. In such cases, it is only required to define the dam outflow equation. On the other hand, if the reservoir already existed, the DEM will likely miss the storage representation (depicting a flat lake area instead). This demands additional bathymetry information (e.g., reservoir level-storage relationships) to correct the model. These two main aspects were added to the MGB framework by Fleischmann et al. (2019a). Open water evaporation and direct precipitation on lake are considered in the same way as for floodplain areas.

In the improved reservoir representation proposed in this paper, this scheme is further developed by comparing different types of reservoir bathymetry representation (Section 2.4) and operation (Section 2.5), which are detailed in the next sections.

2.4 Reservoir storage representation

To improve reservoir storage representation, three different types of reservoir storage/bathymetry representation are compared: (i) a lumped representation of the reservoir storage, by which all storage is concentrated in one only unit-catchment (associated to the dam location), and a distributed method in which the storage is (ii) equally and (iii) variably split among all unit-catchments that compound the reservoir lake, thus allowing the representation of reservoir dynamics. **Figure 2** (bottom panel) presents the schemes for the three simulation methods.

The lumped method (i) ("Lum") consists of concentrating the reservoir stage-volume curve (in this study, provided by the Brazilian National Electric System Operator - ONS) on the unit-catchment holding the dam location. This method is analogous to a level-pool routing method, used in simpler reservoir routing schemes and mainly assuming a horizontal water surface along the reservoir. This approaches a dynamic method (ii and iii) if reservoir length is short, depth is large, inflow hydrograph volume is large, and inflow hydrograph time of rise is long (Fread, 1992). Unit-catchments along the reservoir lake are considered as a river with rectangular cross section, and the downstream boundary condition at the dam location is considered as a simplified uniform flow (a local average slope was adopted in this case).

The equal bathymetry method (ii) ("Eq") consists of equally distributing the volume through the unit-catchments that composes the reservoir. For each level, the reservoir water surface area is equally distributed to the unit-catchments on the reservoir domain through the stage-area relationship. Thus, all the unit-catchments that compose a reservoir have the same storage capacity.

The variable bathymetry method (iii) ("Var") explicitly simulates the reservoir dynamics to improve accuracy in the distribution of reservoir volume across the unit-catchments associated to the reservoir lake. Since the DEM measures the surface water level, there is no information on it about the reservoir bathymetry. Thus, the proposed method estimates the stage-area curve below the reservoir water level (RWL) and combines it with the stage-area curve above the RWL to construct the reservoir actual stage-volume curve, which can be later checked against existing data (in this study, provided by the Brazilian National Electric System Operator - ONS). This method has four steps:

1) Estimation of the stage-area curve above the RWL in a given unit-catchment. This process is automatically obtained using the DEM information within a unit-catchment, by counting the number of cells lower than a specific elevation.

2) Estimation of the "original" river bank elevation in every unit-catchment within the reservoir lake. The "original" riverbanks (i.e., in pristine conditions) were inundated by the dam. Thus, the bank elevation of all unit-catchments that compose the reservoir were defined through a linear interpolation between the bank elevation just downstream of the dam, and the one immediately upstream of the reservoir lake (Equation 3).

$$Z_i = Z_{down} + \left(Z_{up} - Z_{down}\right) \times \left(\Delta X_{down,i} / \Delta X_{down,up}\right) \qquad \text{Equation 3}$$

Where Z represents the bank elevation and ΔX the distance between the river sections. The indices $i, down$ and up represent the sections of the i-th unit-catchment within the reservoir, and the sections immediately downstream to the dam and upstream to the reservoir lake, respectively.

3) Estimation of the stage-area curve for the levels below RWL: it is assumed that the water surface area below the RWL linearly increases with level, and that the water surface area at the river bank elevation is zero. Thus, the stage-area curve below RWL is a line going from an area equal to zero at the river bank elevation (Z_i) to the first point in the stage-area curve above RWL.

4) Matching the estimated reservoir stage-volume curve with the actual one: the reservoir stage-volume is a table relating reservoir volume (V_O) with level (Z). It can be directly compared to the reservoir stage-area curve built with the combination of all the unit-catchments within the reservoir (hereafter Res), which is a table relating area (A_{Res}) to level (Z). In every position j on the stage-area table, a level increment ($Z^j -$

Z^{j-1}) is multiplied by its related reservoir surface water area ($(A_{Res}^{j} + A_{Res}^{j-1})/2$), resulting in an incremental volume (ΔV_{Res}^{j}). Then, the incremental volume observed on the stage-volume curve related to the level Z^{j} ($\Delta V_{O}^{j} = V_{O}^{j} - V_{O}^{j-1}$) is divided by the calculated incremental volume calculated from the stage-area curve (ΔV_{Res}^{j}), generating a volume ratio ($VR^{j} = \Delta V_{O}^{j} \,/\, \Delta V_{Res}^{j}$). The stage-area curve of each unit-catchment (i) within the reservoir is recalculated independently to keep the same incremental volume as the actual stage-volume curve:

$$(a_{Res}^{*\,i,j} + a_{Res}^{i,j-1}) = VR^{j} \times (a_{Res}^{i,j} + a_{Res}^{i,j-1}) \qquad \text{Equation 4}$$

$$a_{Res}^{*\,i,j} = VR^{j} \times (a_{Res}^{i,j} + a_{Res}^{i,j-1}) - a_{Res}^{i,j-1} \qquad \text{Equation 5}$$

Where $a_{Res}^{i,j}$ is the water surface area of the unit-catchment i at the stage-area table position j related to the level Z^{J}. The superscript * indicates the recalculated a values. Equations 4 and 5 indicate an adjustment on the water surface area in level Z^{j} in order to preserve the incremental volume indicated by the actual stage-volume curve.

This process is repeated through all levels ($Z^{1}\ to\ Z^{n}$) of the stage-volume curve, modifying the stage-area curve of each unit-catchment within the reservoir.

2.5 Reservoir operation

The dam release is set as an internal boundary condition of the hydrodynamic model (MGB), by replacing Equation 1 by a dam outflow equation. Three types of operation schemes are compared here, considering two different approaches each: one based on regionally available data, and another with global-based parameterization. The

three operation types are representative of different approaches that have been implemented in state-of-the-art modeling systems, from generic to data-driven ones, described as follows.

2.5.1 Reservoir operation schemes H06 and H06Glob

This is a generic, inflow-based operation based on the equation proposed by Hanasaki et al. (2006) and adapted by Shin et al. (2019). This operation considers that the dam outflow is a simple function of the inflow modulated by the dam regulation capacity and the storage at the beginning of each hydrological year. Here, it is used at a daily basis and for hydropower plants, so that it does not take into account downstream water demands for irrigation or other uses. Dam outflow is defined by Equation 6:

$$Q(i,t) = R_i K_{i,y} I_m + (1 - R_i) I_{t-1} \quad \text{Equation 6}$$

Where $Q(i,t)$ is the ith dam outflow at the time step t, R_i a regulation capacity constant that can be calibrated with observations or estimated with Equation 7 (Shin et al., 2019), I_m and I_{t-1} the annual average and dam inflow, respectively, and $K_{i,y}$ the storage fraction at the beginning of the hydrological year (Equation 8). The hydrological year of each dam is defined as the month where the naturalized flow becomes lower than the average (i.e., the beginning of the drawdown season) (Hanasaki et al., 2006).

$$R_i = \min(1, \alpha c_i) \quad \text{Equation 7}$$

$$K_{i,y} = S_{first,y} / \alpha C_i \quad \text{Equation 8}$$

The term c_i is the ratio between the reservoir maximum storage C_i and the annual average dam inflow ratio ($c_i = C_i / I_m$), $S_{first,y}$ is the storage at the beginning of

each hydrological year y, and αC_i is the target storage, where α is a constant set to 0.85 following Hanasaki et al. (2006).

Scenario H06 estimates R from a calibration procedure based on regionally available observations, while scenario H06Glob (global) adopts equation (6) for estimating R.

2.5.2 Reservoir operation schemes 3PT and 3PTGlob (Three-point rule curve)

This is a target storage-and-release-based rule (Yassin et al. (2019), consisting of a three-point rule built upon simple dam characteristic parameters, as minimum and maximum operational levels, and maximum discharges (**¡Error! No se encuentra el origen de la referencia.**a). Similar approaches were adopted by Zajac et al. (2017) and Yassin et al. (2019). This operation emulates a reservoir rule curve that is constant throughout the year with outflow as a linear function of water level, guided by three points. The regional approach (scenario 3PT) adopts the following points based on actual dam information (i.e. observations): minimum operational level (for which outflow is zero), average operational level (for which outflow is obtained from the average observed outflow), and maximum design level (associated to the dam design discharge). Supplementary Material S1 presents the adopted parameters for all dams. Scenario 3PTGlob (global approach) follows Zajac et al. (2017), and adopts the percentiles 0.1, 0.3 and 0.97 for the minimum (conservative), normal, and maximum (flood) storages, which are associated to the 5th, 30th, and 97th percentiles of naturalized daily discharge, respectively.

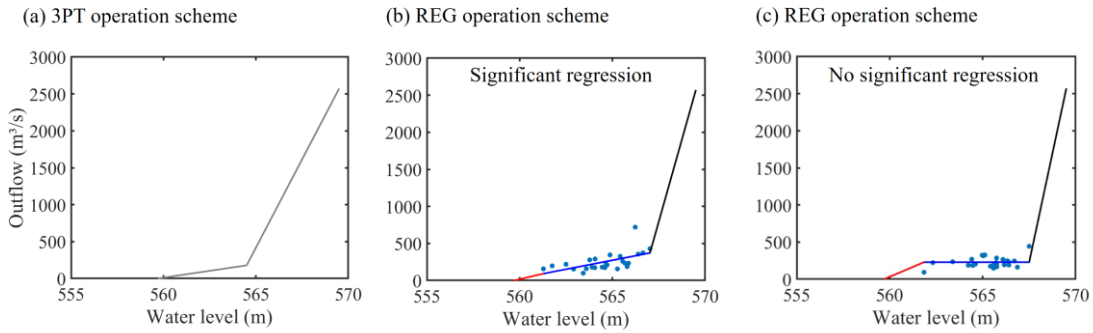

419

420 **Figure 3**. Reservoir operation exemplified for the Jurumirim Dam (ID 1 in **Figure 1**), for the (a)
421 operation scheme '3PT', considering only three pre-defined points related to dam characteristics
422 (water level and design discharges), (b) 'REG' scheme, with significant regression between
423 observed monthly mean water level and dam outflow obtained for the month of December, and
424 (c) 'REG' scheme, without significant regression for the month of September. The blue dots
425 represent observations, and the lower (upper) extrapolation of the reservoir operation for ranges
426 out of observations is depicted in red (black). See description of the operation schemes in the
427 text (Section 2.5).

428

429 2.5.3 Reservoir operation schemes REG and REGGlob (Regression-based rule)

430

431 This is also a target storage-and-release-based rule based on a data-intensive
432 approach (**¡Error! No se encuentra el origen de la referencia.**b and **¡Error! No se**
433 **encuentra el origen de la referencia.**c). Linear regressions are computed between
434 observations of monthly average water levels and dam outflows, so that it emulates a
435 rule curve for each month of the year following the actual operation (Oliveira and
436 Loucks, 1997). A similar operation was investigated by Solander et al. (2016). For each
437 month, positive relationships are adopted as those with Pearson correlation higher than
438 0.4, which is considered satisfactory based on a visual inspection (**¡Error! No se**

encuentra el origen de la referencia.b). For non-positive relationships (**¡Error! No se encuentra el origen de la referencia.**c), the monthly average discharge was used for all simulated days for a given month. For water levels out of the observed range for a given month, dam characteristics related to minimum operational level (for which outflow is zero), and maximum design level (dam design discharge) were adopted, and linearly interpolated with the observed ranges.

The global approach (scenario REGGlob) adopts long term outflow average instead of monthly regressions, making the operation similar to the standard operating policy (SOP) (Draper and Lund, 2004), considering the long term streamflow as the demand.

2.6 Model application in the Upper Paraná River Basin

The model was applied to the Upper Paraná River Basin with daily time step for the period 1st Jan 1979 to 31st Dec 2015 (35 years + 1 spin-up year). It was run with in-situ daily precipitation from 2030 gauges from the following institutions: Brazilian National Water Agency (ANA), Water Resources Agency of Argentina (BDHI) (http://bdhi.hidricosargentina.gov.ar/) and National Meteorological and Hydrological Service of Paraguay (DMH) (https://www.meteorologia.gov.py/). Details on precipitation data interpolation to model units are provided in Supplementary Material S2. Long term climate averages from 195 stations of the Brazilian National Institute of Meteorology (INMET, available at <http://www.inmet.gov.br/>) were used to compute evapotranspiration.

Drainage network and unit-catchments (total of 9625 units with 10 km long river reaches) were derived from the 90 m Hydrosheds SRTM DEM (Lehner et al., 2008) with the IPH-HydroTools GIS toolkit (Siqueira, et al., 2016a). Hydrologic Response Units (HRU's) were used to define homogeneous regions for the rainfall-runoff parameters, and were derived from the South America HRU map developed by Fan et al. (2015). Model parameters related to soil, vegetation and river hydraulics (bankfull width and depth from geomorphic relationships, and Manning's roughness coefficient) are further discussed in Supplementary Material S2.

The model was calibrated (validated) for the period 1990-2010 (1980-1990) with 143 in-situ discharge gauges from ANA considering the pristine scenario (i.e., without reservoirs). Naturalized flows from ONS were considered for gauges downstream of dams. Supplementary Material S2 presents details on the model adjustment, including performance metrics and simulated hydrographs. Overall, the model satisfactorily represented natural discharges basin-wide, with 78% (79%) of the evaluated gauges with Nash-Sutcliffe (Log Nash-Sutcliffe) metric > 0.6 for the validation period, and 42% of the gauges with the absolute value of bias < 10%.

The 30 regulation dams within SIN were considered, in addition to Itaipu dam (a run-of-river dam but very relevant in terms of size and energy production) (**Figure 1**). For simplicity, all other run-of-river reservoirs were not considered in the simulations, since our focus was on dams with regulation capacity. To properly address basin-wide flow regulation, the dams were only considered after their year of inauguration, so that the model simulated the dam first filling. The effects of reservoirs were not used for model calibration, but only considered for the scenarios presented in the following Section 2.7.

2.7 Experimental design

A total of 12 simulation scenarios were run, considering the different reservoir bathymetry representation and reservoir operation schemes (**Table 1**). The performance of a given reservoir simulation was first assessed in terms of discharge and active storage for all dams. Observed time series of active storage and dam outflows were obtained from ANA (https://www.ana.gov.br/sar/). The hydrodynamics was assessed in terms of the water surface elevation longitudinal profile at Itaipu dam, by comparing simulations with satellite altimetry estimates from the ICESat mission (Schutz et al., 2005). ICESat carries a LiDAR sensor and has a maximum inter-track distance of 30 km and a repeat cycle of 91 days. A basin scale assessment was also made by computing, for each river reach, the root mean squared deviation (RMSD) between simulated water levels under scenarios Lum, Eq and Var (**Table 1**).

Model performance for discharge was assessed with Nash-Sutcliffe (NSE), normalized root mean squared error (NRMSE) of peak discharges, and relative errors in high (Q_{10}, i.e., discharge that is exceeded 10% of the time) and low flows (Q_{90}). For reservoir active storage, NRMSE and Pearson correlation metrics were adopted. Finally, the average peak attenuation for each dam was assessed by first computing the discharge reduction between dam inflow and outflow for each of the dam's maximum annual events, followed by estimation of the average of the annual values. The simulated peak attenuation was compared to the observed one with the NRMSE metric.

In addition, the role of the online coupling between hydrology and hydrodynamic processes was tested by performing tests with and without coupling in Section 3.1. The

simulation without coupling was performed by considering that evapotranspiration only occurs from the non-flooded soil/vegetation system, i.e., reservoir open water evaporation is not considered into the evapotranspiration computation.

Since there is high uncertainty on the estimation of the active flow width (B in Equation 1) along the reservoir when it is simulated in a distributed way (i.e., reservoir storage types Eq and Var; Section 2.4), hydrographs are presented in Section 3.1 considering two types of computation: (i) adopting the original channel width estimated from geomorphic relationships, and (ii) considering the active width for unit-catchments within reservoirs as the unit-catchment flooded area divided by its length (10 km), i.e., considering that there is active flow along the whole reservoir cross section area.

Finally, the developed regional scale hydrodynamic model was used to investigate the relative role of floodplains and reservoirs on flood attenuation. This was carried out following the approach by Fleischmann et al. (2019a), where the model was run with three river/floodplain scenarios: (i) pristine flow scenario (naturalized flow; with floodplains but without reservoirs); (ii) without both floodplains and reservoirs, where cross sections were assumed always rectangular and thus disregarding floodplain topography; and (iii) with both floodplains and reservoirs. The role of reservoirs on flood attenuation was estimated by computing the peak attenuation between scenarios (i) and (iii) for the maximum flood event of each simulation year. The role of floodplains was similarly computed, but considering the difference between scenarios (ii) and (i). Table 1 summarizes the model runs.

Table 1

Reservoir simulation scenarios.

Reservoir operation*	Storage representation**	Scenario	Operation details
H06	Lum	H06Lum	R calibrated
H06	Eq	H06Eq	
H06	Var	H06Var	
H06Glob	Var	H06GlobVar	R estimated as $\min(1, \alpha c_i)$
3PT	Lum	3PTLum	Minimum, normal and maximum levels and outflows derived from dam characteristics
3PT	Eq	3PTEq	
3PT	Var	3PTVar	
3PTGlob	Var	3PTGlobVar	Minimum, normal and maximum levels and normal and maximum outflows estimated as simple percentiles as proposed by Zajac et al. (2017)
REG	Lum	REGLum	Monthly linear regressions between level and outflows; months with low correlation use monthly average outflow instead
REG	Eq	REGEq	
REG	Var	REGVar	
REGGlob	Var	REGGlobVar	Annual average outflow used for all months

* Reservoir operation: H06 (based on Hanasaki et al. (2006)), 3PT (three-point rule curve), REG (regression-based operation). "Glob" refers to the global parameterization of each operation type.

** Reservoir storage representation types: Lumped (Lum), Equal bathymetry (Eq), Variable bathymetry (Var).

3 Results

3.1 Effects of reservoir storage representation

This section presents the results and differences in the reservoir dynamics according to the storage representation approaches (Lum, Eq, Var). While all schemes yielded similar estimates of dam outflows, as exemplified for a few dams in **Figure 4**a, some key differences were identified. In some cases, the lumped method led to a discharge attenuation in relation to the other two methods (smaller and delayed peaks). This is due to the typical approach adopted on large-scale hydrological modeling in the lumped (offline) simulation, i.e., using as inflows the simulated discharges at the dam location, instead of computing the inflows as the modeled flows at the river reaches close to the most upstream reservoir lake area. This approach causes the flood wave to be routed along the reservoir as it was a river reach, adding artificial routing along the drainage network. Hence, for lumped model applications, it is best to select all tributaries that drain into the reservoir (along with direct lake inputs) and consider it as the dam inflow. This effect was clearer for Itaipu dam, which is located in the lower part of the basin, integrating the effects of all upstream dams and having a long reservoir.

Our results show that simpler, lumped reservoir models can simulate downstream discharge similarly to dynamic and distributed ones (**Figure 4**a). However, the lumped method fails to represent backwater effects when compared to the distributed methods (Equal and Variable bathymetry) (**Figure 5**a). High deviation among Lum and Var scenarios (RMSD > 10 m for some reservoirs) occurs for most reaches upstream from dams.

As a validation experiment, ICESat satellite altimetry data were used to assess the simulated profile of water surface elevation along Itaipu reservoir under the three different storage schemes (**Figure 5**b). The lumped method is unable to simulate it properly, and the slope in the upstream part of the lake was better represented with the Var method. An intermediate behavior was obtained with the Eq method. Although this method considers the reservoir to behave as a large box with horizontal water level, the lake is assumed as connected to the rest of the drainage network, and thus the method is capable to represent backwater.

On the other hand, the actual level in the lake area closer to the dam is more dependent on the dam operation, and its simplification led to higher errors in the estimated Itaipu reservoir storage. For instance, the low water level in Oct/2003 (lake level closest to the dam at 216.6 m; **Figure 5**b) is related to the low simulated active storage (around 14 km³; see **Figure 6**d in next section), while actual values were around 219.3 m for level and 18.1 km³ for storage. Itaipu is also a large dam (~170 km long), and its lake is composed of many unit-catchments (which are 10 km long).

The hydrographs presented in **Figure 4**a also compare different ways of representing flow width in the distributed reservoir simulation (bold lines), as well as scenarios with and without reservoir open-water evaporation (i.e., not considering an online hydrologic-hydrodynamic coupling; dashed lines). Downstream discharges had mostly similar values, indicating a low sensitivity to both flow width conceptualization and the online coupling scheme.

Regarding evapotranspiration estimates, differences among Lum, Eq and Var scenarios would arise if reservoir flooded areas were largely divergent, but this difference was relatively small in comparison to other model uncertainties. Our estimations of reservoir evaporation rates are in agreement with other studies in the

Paraná Basin (Bueno et al., 2016). Looking at the basin scale, we estimated an increase of annual ET rates by 15 mm/year due to existence of reservoirs. The net reservoir evaporation (i.e., reservoir evaporation minus the evapotranspiration that would occur without the lake, which is equal to the difference between blue and red lines in **Figure 4**b) for the assessed lakes varied between 21±12 mm/month (mean±SD) for Itaipu and 70±41mm/month for Itumbiara (located in the north of the basin; ID 19 in **Figure 1**). This loss can be relevant during dry periods, and thus must be accounted for in large scale models. For instance, loss in energy production due to reservoir evaporation in the Brazilian southeast region was estimated as 2% (over 900 MW; Zambon et al., 2018), and it is also an important measure to assess regional scale reservoirs' water footprint (Semertzidis et al., 2019). At Itumbiara dam, the modeled evapotranspiration was highly constrained by soil moisture during austral winter, what explains the large net evaporation losses. This difference led to a higher peak simulated under the scenario without open water evaporation (**Figure 4**a). When looking at finer scales, evapotranspiration rates will drastically differ. Since the lumped (offline) method is not able to represent the dynamic conversion between dry and flooded soil/vegetation, the representation of local scale coupled processes between surface and atmosphere will perform poorly, as well as the local scale runoff estimation.

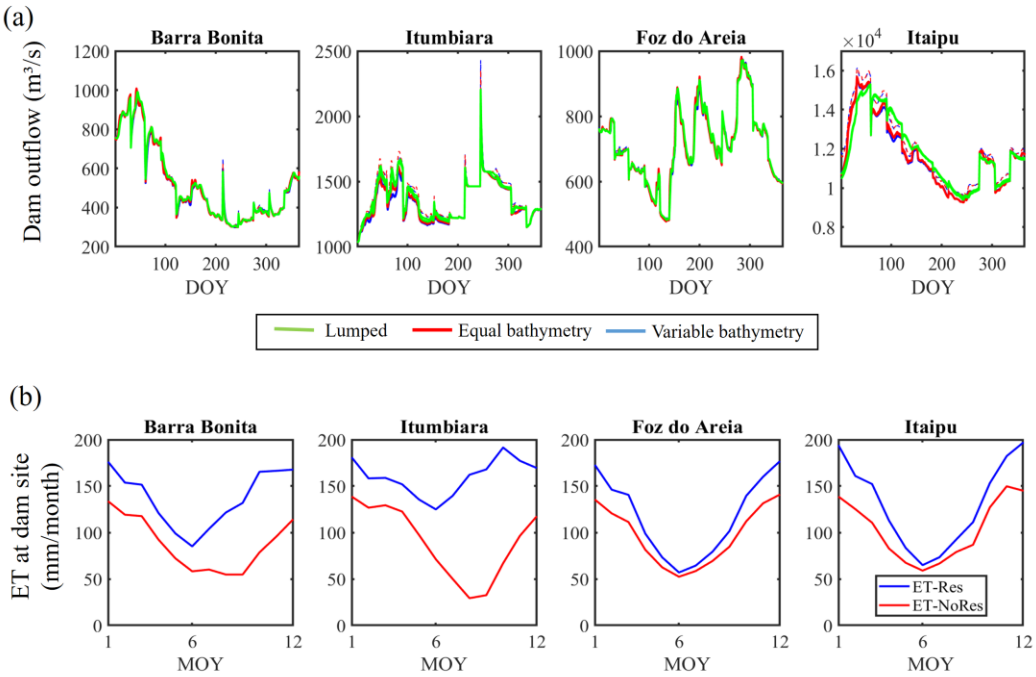

609

610 **Figure 4**. (a) Daily climatology of simulated dam outflows for the three types of storage representation
611 (Lumped, Equal bathymetry, Variable bathymetry) and for Barra Bonita (ID 3 in **Figure 1**), Itumbiara
612 (ID 19), Foz do Areia (ID 15) and Itaipu (ID 18) dams. Results adopt the operation R. Bold colors refer to
613 default scenarios with two different flow width values (which converge to very similar values), while
614 dashed lines with light colors are scenarios not computing reservoir open water evaporation. (b) Monthly
615 climatology of open water evaporation (ET-Res; Penman equation) and evapotranspiration without
616 reservoir effects (ET-NoRes; i.e., Penman-Monteith equation not considering reservoir surface area) at
617 the location of the dam sites. The operation scheme REG is adopted for all plotted results.

618

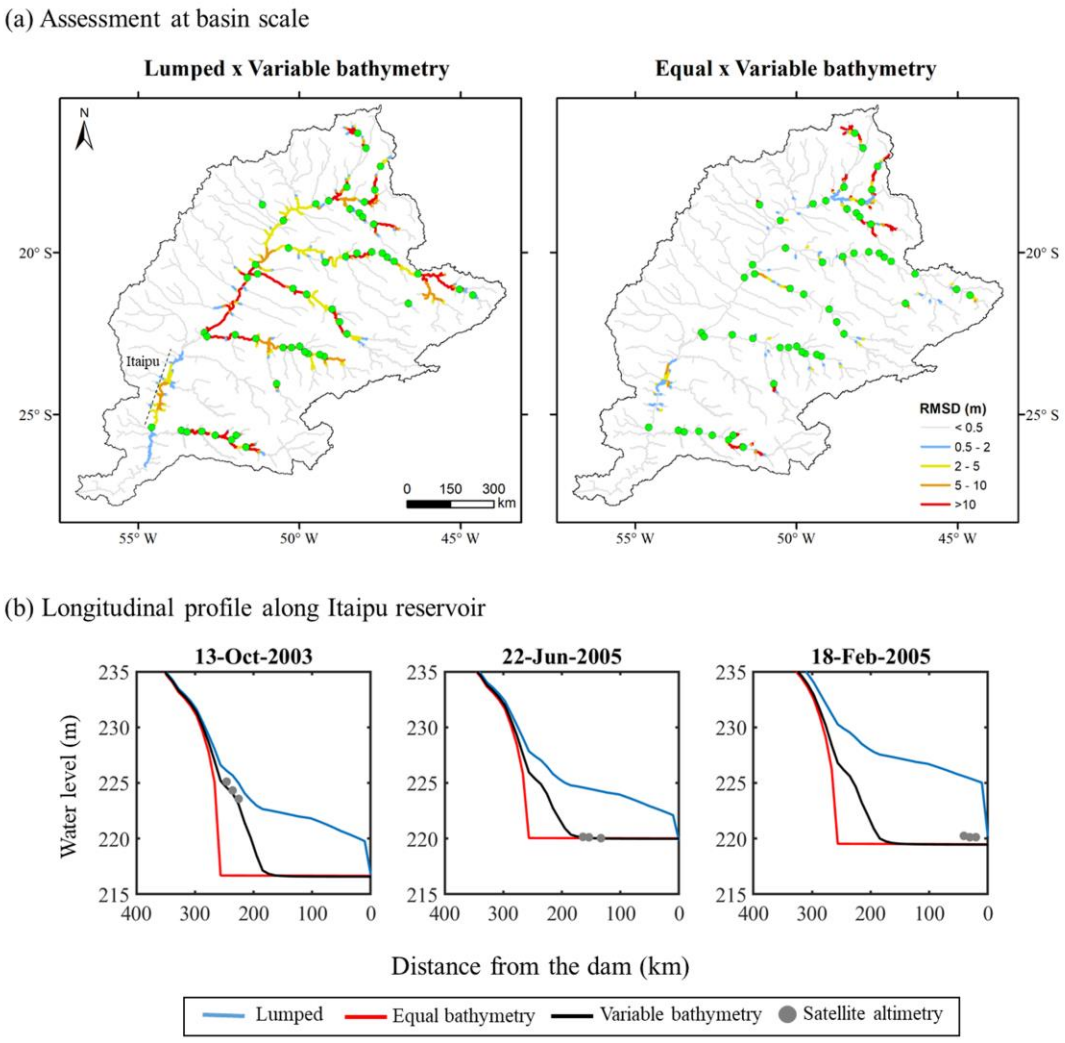

619

620 **Figure 5**. (a) Spatial assessment of RMSD regarding simulated water level, for scenarios lumped x
621 variable bathymetry (left column) and equal x variable bathymetry (right column). Higher RMSD values
622 indicate higher discrepancy between storage representation types to estimate backwater effects. Green
623 circles refer to the simulated dams. (b) Validation of the simulated longitudinal water level profile along
624 Itaipu reservoir with ICESat altimetry data for three different dates. The Itaipu reservoir lake area is
625 highlighted in the panel a. The operation scheme REG is adopted for all plotted results.

626

627

628

3.2 Effects of reservoir operation

This section compares the different reservoir operation (H06, 3PT, REG, in order of increasing data requirement) and storage/bathymetry representation schemes (Lum, Eq, Var), addressed in terms of dam outflow and reservoir hydrodynamics. The differences among the simulated operation schemes are larger than among the reservoir bathymetry types for discharge and active storage estimation (**Figure 6** and **Figure 7**).

Results for the same four dams analyzed in the previous section show that the REG operation scheme led to far better outflow estimation for Itumbiara and Itaipu dams. In these cases, operations H06 and 3PT also outperformed the natural flows scenario (i.e., without reservoir effects). The overall model performance in representing basin-wide hydrologic regime alteration (as depicted by Itaipu dam) shows that the best performance was obtained for REG (NSE 0.69), followed by H06 (0.47) and 3PT (0.19), and that all of them outperformed the scenario without dams (-0.26). For Itumbiara, the better performance of REG for outflow compared to the other scenarios can be seen in the better depicted seasonality, also reflected on the storage simulation. For Foz do Areia dam, located in a river with low precipitation seasonality, all model versions led to similar estimates as the natural flow scenario, i.e., the inclusion of reservoirs did not lead to improvements. The simulation performance for active storage (NRMSE) was similarly satisfactory for the four dams and all scenarios, except for Itaipu under operation REG, which outperformed the others by significant margins (9% for REG, against 23% and 27% for H06 and 3PT, respectively).

A similar behavior was observed when looking at the ensemble of 31 dams (**Figure 7** and **Figure 8**), which was supported by a basin-wide assessment for the whole drainage network (Supplementary Material S3). The highest differences were obtained for NSE,

where REG had the best performance, followed by H06 and 3PT, and for active storage r, for which REG was followed by 3PT and H06. Indeed, a more satisfactory performance was expected for REG given its more data-intensive nature. The three-point rules (3PTLum, 3PTEq, 3PTVar and 3PTGlobVar) had the lowest performance for discharge in terms of NSE, but this was not the case for high (Q_{10}) and low flows (Q_{90}) and peak discharges. Interestingly, for low flows, all operation types were outperformed by the natural flow scenario, showing that the tested operations led to excessive discharge attenuation (i.e., overestimated base flows) during dry periods.

The operation scheme REG, which relies on observed data, provided the best discharge estimates with a median NSE of 0.3 and a maximum of 0.75 for the 31 reservoirs. Although the basin-wide hydrological alteration was relatively well captured, e.g., at Itaipu dam location (**Figure 6**), the non-data intensive schemes (H06 and 3PT) need further improvements if aiming at locally relevant estimates of dam operation.

The analysis of regional (H06, 3PT, REG) versus global-based parameterizations (H06Glob, 3PTGlob, REGGlob) showed that the global ones had a relatively poorer performance in relation to their regional counterparts. For instance, the regression with monthly values (REGGlob), considering long term averages as outflow, presented the poorest performance for peak NRMSE and high and low flows, while 3PTGlobVar scenario presented the poorest representation of active storage. However, for certain purposes these global approaches could already provide valuable discharge estimates, e.g., for providing a general understanding of regional scale hydrological alteration. For example, median NSE values were 0.1 (0.1) for scenario H06 (H06Glob), and 0.3 (0.1) for REG (REGGlob), showing the just slightly better performance of the regional parameterization. The global setups were also more accurate than naturalized flows for all metrics except for low flows.

There was an overall satisfactory model performance to estimate peak attenuation, with Pearson correlation between 0.72 and 0.91, and NRMSE between 10% and 22% (**Figure 8**). The different types of storage representation led to very similar NRMSE values between simulation and observation, and the same occurred for the reservoir operation, although H06 was slightly better than 3PT, which in turn was marginally better than REG. This is interesting given the low degree of data requirement in the H06 scheme. The global-based parameterization led to less accurate results for scenarios H06Glob and REGGlob, but not for 3PTGlob, in relation to their counterparts H06, REG and 3PT. Among all assessed metrics in **Figure 7**, the only one for which a noticeable difference was obtained regarding storage representation was the correlation of peak attenuation, for which the variably distributed storage (Var) yielded better values than the other ones.

The capability of the dams' regulation capacity (total active storage divided by long term average discharge; red to blue colors in **Figure 8**) to predict peak attenuation was also investigated. A positive trend between regulation capacity and peak attenuation was clearer for REG (i.e., lower attenuation values with red color and higher ones with blue). The lack of a clear relation resulted from the behavior of the three dams with largest regulation capacity (Serra do Facão, Nova Ponte and Emborcação dams; ID's 30, 24 and 14 in **Figure 1**, respectively), which were associated to a relatively small peak attenuation (around 10%).

Finally, the dry years of 2000-2001 provide a stress test for our modeling system. During this period, a major drought affected the Brazilian hydropower system, which is associated to delays in generation investment leading to a large energy crisis in the country (Jardini et al., 2002). In Jan/2000, Itaipu and Barra Bonita (ID 3 in Figure 1) dams reached their lowest levels (observations available since 1993). The same

occurred for Itumbiara in Nov/2001. Among the four analyzed reservoirs in **Figure 6**, only Foz do Areia, located in the Brazilian southern region, did not have an extreme year during this period. The REG scenario was able to satisfactorily simulate some of dams' drawdowns, but there was no clear pattern among the representation of this extreme year: this scheme estimated a too high (small) drawdown for Itaipu (Itumbiara) dam, but yielded satisfactory estimates for Foz do Areia and Barra Bonita dams.

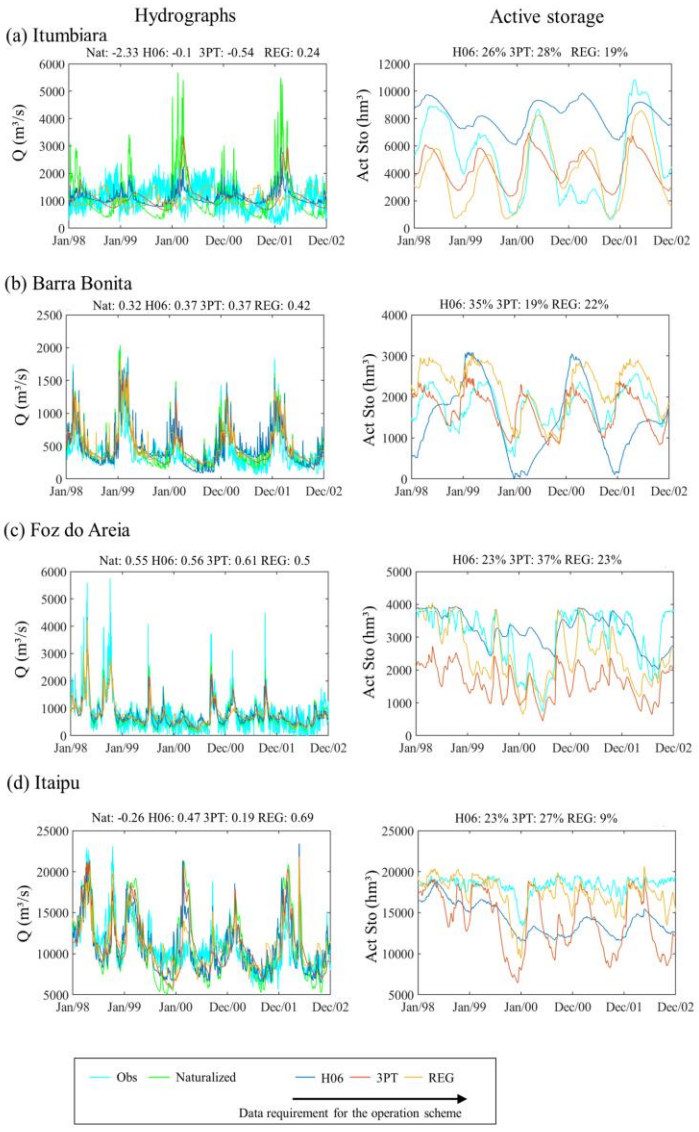

Figure 6. Simulated dam outflow (Q) and active storage (Act Sto) for the different operation types (H06, 3PT, REG), with the variably distributed reservoir simulation method, for four dams (Itumbiara, ID 19 in

Figure 1; Barra Bonita, 3; Foz do Areia, 15; and Itaipu, 18). NSE and NRMSE performance metrics for each scenario are presented for discharges (left column) and storage (right column), respectively. Pristine simulated flows (i.e., without dams; "Nat") are also presented. The unit "hm³" stands for cubic hectometers (i.e., 10^6 m³).

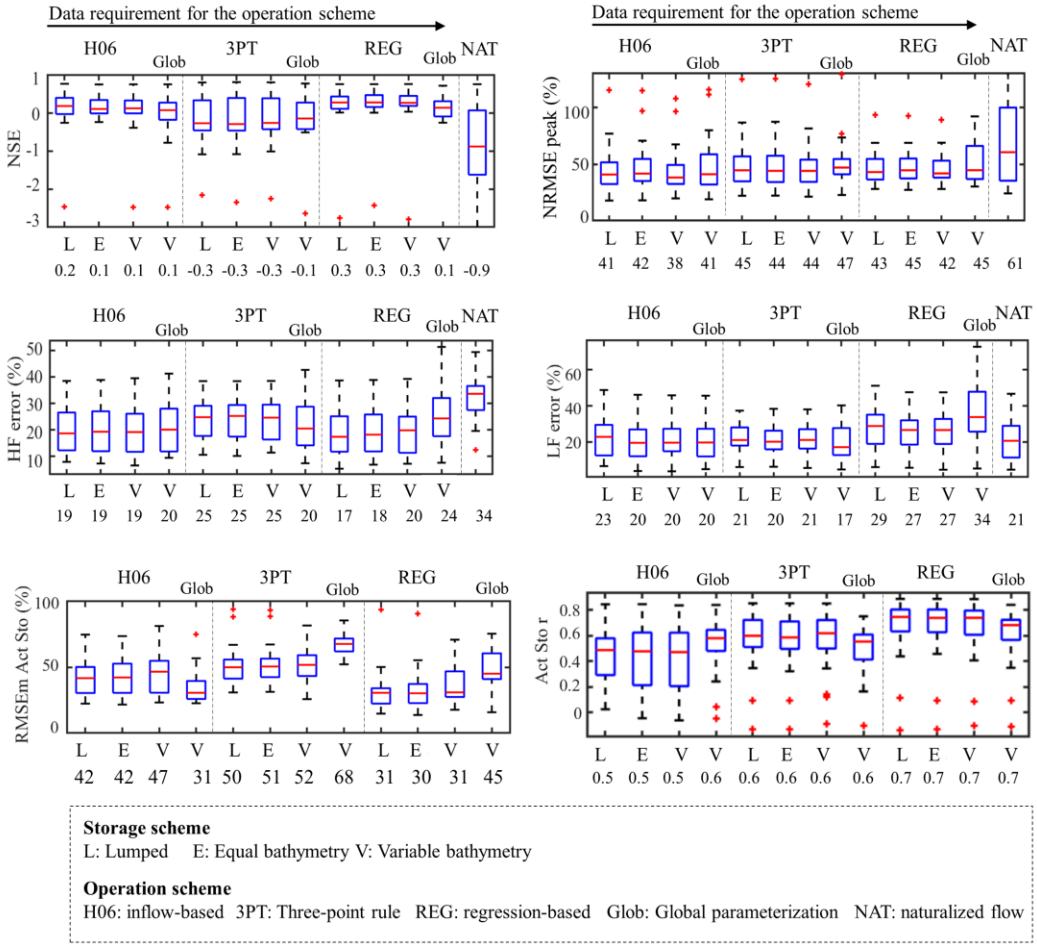

Figure 7. Model performance for discharge (NSE; NRMSE of peak discharges; and errors in high (HF) and low flows (LF)) and active storage (NRMSE and r) for the 12 scenarios of operation types and reservoir simulation methods (**Table 1**), as well as for the naturalized (pristine) flow scenario (Nat; for discharge analysis only). Results are presented as boxplots containing values of the 31 simulated dams, and the metric median values are presented below the scenario names. From left to right, the operation schemes are ordered in terms of increasing data requirement.

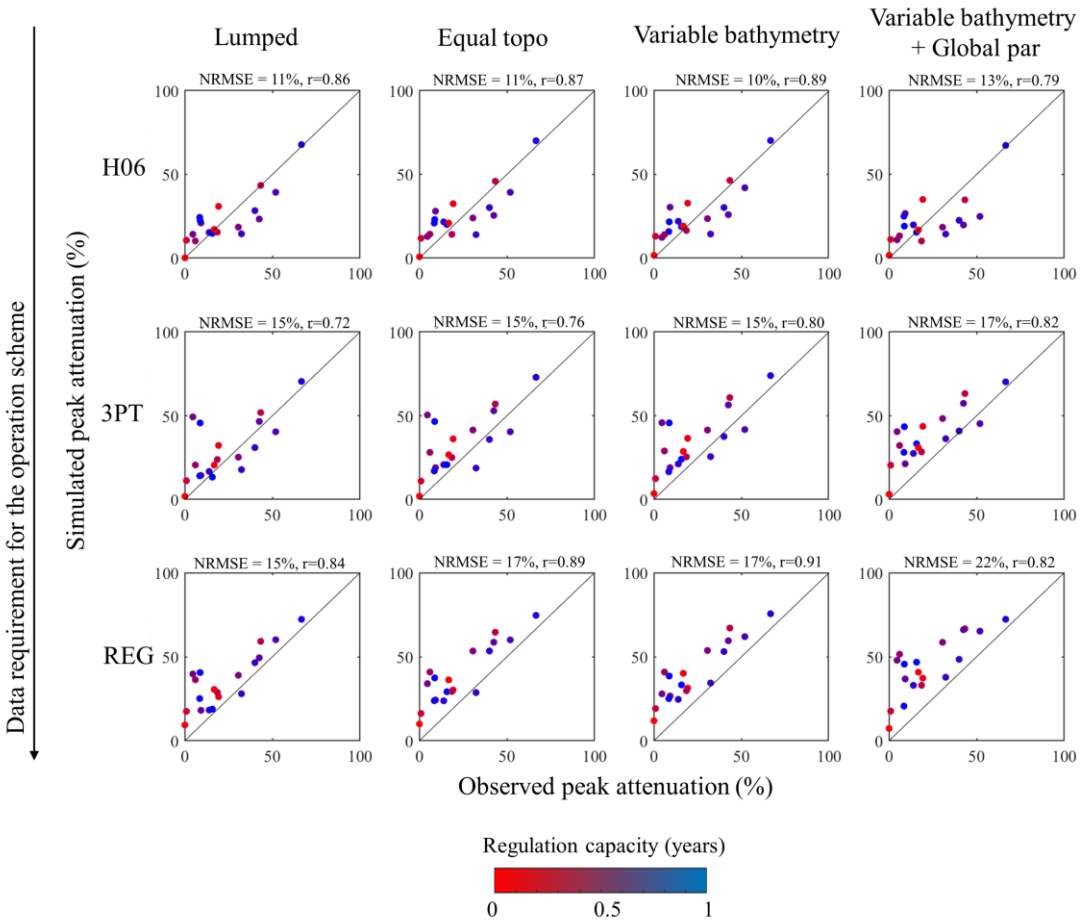

727

728 **Figure 8**. Comparison between observed and simulated peak attenuation for each of the 12 scenarios.
729 Each row refer to a reservoir operation scheme (H06, 3PT, REG, with and without global
730 parameterization – Global par), and each column to a storage representation scheme (Lumped, Equal
731 bathymetry, Variable bathymetry). Each point refers to a simulated dam, and colors refer to the dam
732 regulation capacity (total active storage divided by long term average discharge, in years).

733

734 ### 3.3 The relative role of floodplains and reservoirs on flood attenuation

735

736 River-floodplain-reservoir hydrodynamic models have been used to understand
737 the effects of reservoirs on downstream flooding (Fleischmann et al., 2019a; Mateo et
738 al., 2014; Pokhrel et al., 2018; Shin et al., 2019, 2020). Here we follow the methodology
739 proposed by Fleischmann et al. (2019a) and use the developed MGB model structure,

740 with distributed representation of reservoir bathymetry and a fully coupled river-
741 floodplain-reservoir scheme, to investigate the relative role of natural floodplains and
742 reservoirs on flood attenuation along the Upper Paraná Basin. Generally, natural
743 floodplains and reservoirs have a complementary role on flood attenuation in the basin.
744 While floodplains are more important along tributaries' headwaters (e.g., Iguaçu,
745 Paranapanema, Grande and Ivinhema rivers) and in the lower reaches of the Paraná
746 mainstem, reservoir effects are more relevant along medium to lower reaches of
747 tributaries (**Figure 9**). Part of the reservoirs' storage is currently allocated for flood
748 control during the wet season (Oct-Apr), following the coordinated operation of the
749 Paraná dam cascades (ONS, 2019).

750 Located along the Paraná mainstem, the 230 km floodplain between Porto
751 Primavera and Itaipu dams is known as the last natural large wetland in the Upper
752 Paraná Basin (see **Figure 1** for location), with important ecosystem processes relying on
753 it (Agostinho et al., 2001). The flood storage along this area leads to major discharge
754 attenuation that is propagated downstream, and it is fundamental for flood control in
755 benefit of both Itaipu dam and riverine cities. If the reservoirs did not exist, the reaches
756 flooded by the reservoir lakes would provide additional storage along the floodplain.

757 The comparison between scenarios with and without floodplains shows that the
758 magnitudes of maximum flows are likely to be largely overestimated if basin-wide
759 floodplain storage is not considered (**Figure 9**b). For instance, for the Iguaçu River at
760 Fluviópolis, ignoring this effect would lead a 10-yr flood to be estimated as 6,000 m^3/s
761 (green dots in **Figure 9**b) instead of 3,000 m^3/s (blue and red dots). The effect of
762 upstream floodplains propagate downstream (**Figure 9**a), although they affect the lower
763 reaches of only a few tributaries (e.g., Iguaçu river, with attenuation > 20% for all
764 reaches along the river mainstem). Simulated and observed hydrographs at Água

765 Vermelha and Itaipu dams also stress the role of floodplains and reservoirs on discharge
766 alteration, for both high and low flows. The large effect of floodplains relates to the
767 difference between green and black lines in **Figure 9**b. Furthermore, the major role of
768 reservoirs on flood attenuation along main rivers makes their representation
769 fundamental to correctly estimate flood frequencies in the downstream reaches.

770 Finally, performing an online, fully coupled simulation of the river-floodplain-
771 reservoir continuum allows a continuous representation at the regional scale of the
772 spatial-temporal variation of hydraulic variables as water levels. It is exemplified for the
773 Iguaçu river mainstem, a major southern tributary of the Paraná (**Figure 10**).
774 Longitudinal (maximum and minimum) water surface elevation profiles, as well as
775 maximum flooded areas, highlight the connected hydrological-hydraulic processes that
776 occur basin-wide. Along the Iguaçu, major floodplains occur in the upper reaches, from
777 the most upstream parts close to Curitiba city (detail iii in **Figure 10**b), to União da
778 Vitória and Fluviópolis cities (see **Figure 9**b and detail ii in **Figure 10**b). A geologic
779 control creates valleys with rapids between floodplains, setting up hydraulic controls
780 and increasing upstream floodplain storage. União da Vitória is also affected by
781 backwater effects from Foz do Areia dam, located a few kilometers downstream. In this
782 study we only simulated regulation dams, while run-of-river ones were not considered
783 and thus are not represented in the simulated water surface elevation continuum.
784 Downstream of the cascade, the Iguaçu has again an incised valley with small
785 floodplains, and the river width is controlled by the hydraulic control of the large Iguaçu
786 Falls (detail i in **Figure 10**b). This example reinforces the model capability to represent
787 the coupled human-water system at regional scale.

788

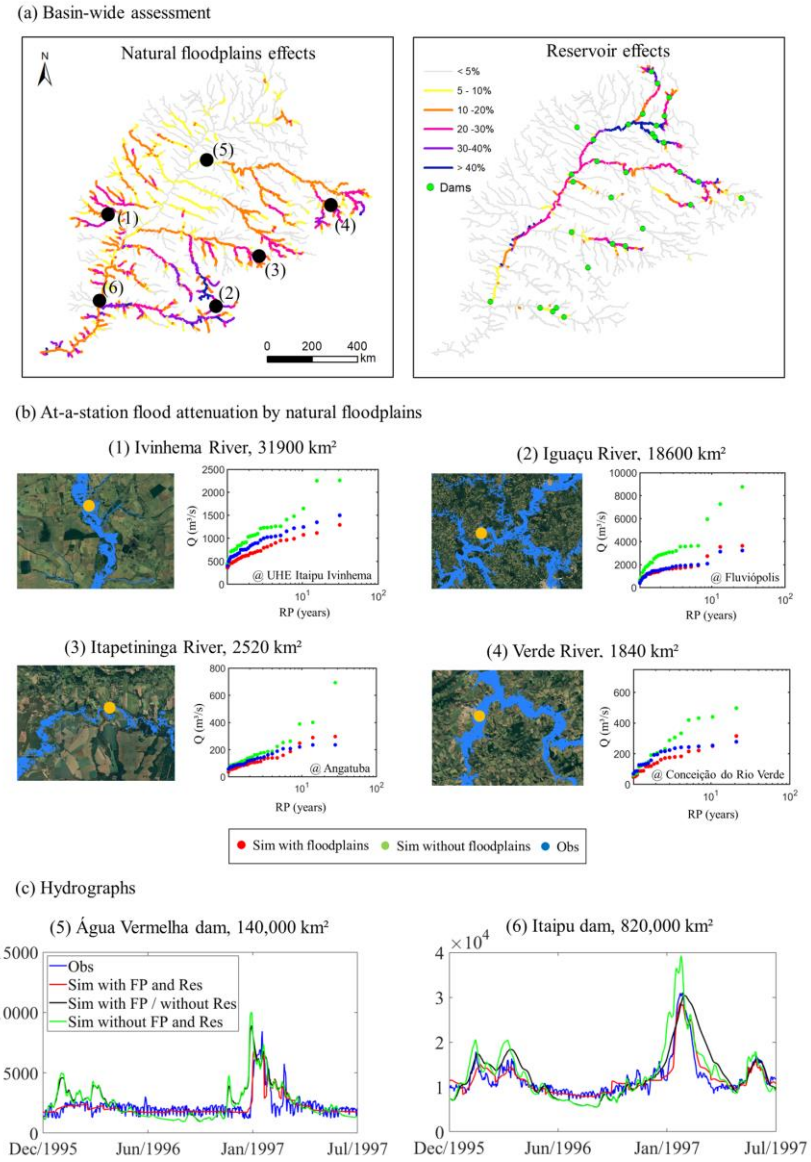

Figure 9. (a) Relative role of floodplains and reservoirs on flood attenuation, in terms of average attenuation of maximum annual events. The H06Var reservoir simulation scenario is adopted because of smallest peak attenuation NRMSE. (b) At-a-station assessment of flood attenuation by floodplains at four locations in upstream tributaries (location in figure a), in terms of simulations with and without floodplains, and observed (Obs) maximum annual discharges (flood frequency analysis). Maximum simulated flood extents are presented as blue areas in the left figures, together with Google Earth imagery and the location of the gauges (yellow). (c) Simulated and observed hydrographs at Água Vermelha and Itaipu dams (location

in figure a) for different scenarios of floodplains (FP) and reservoirs (Res). The REGVar simulation scenario is used here because it led to the highest discharge NSE.

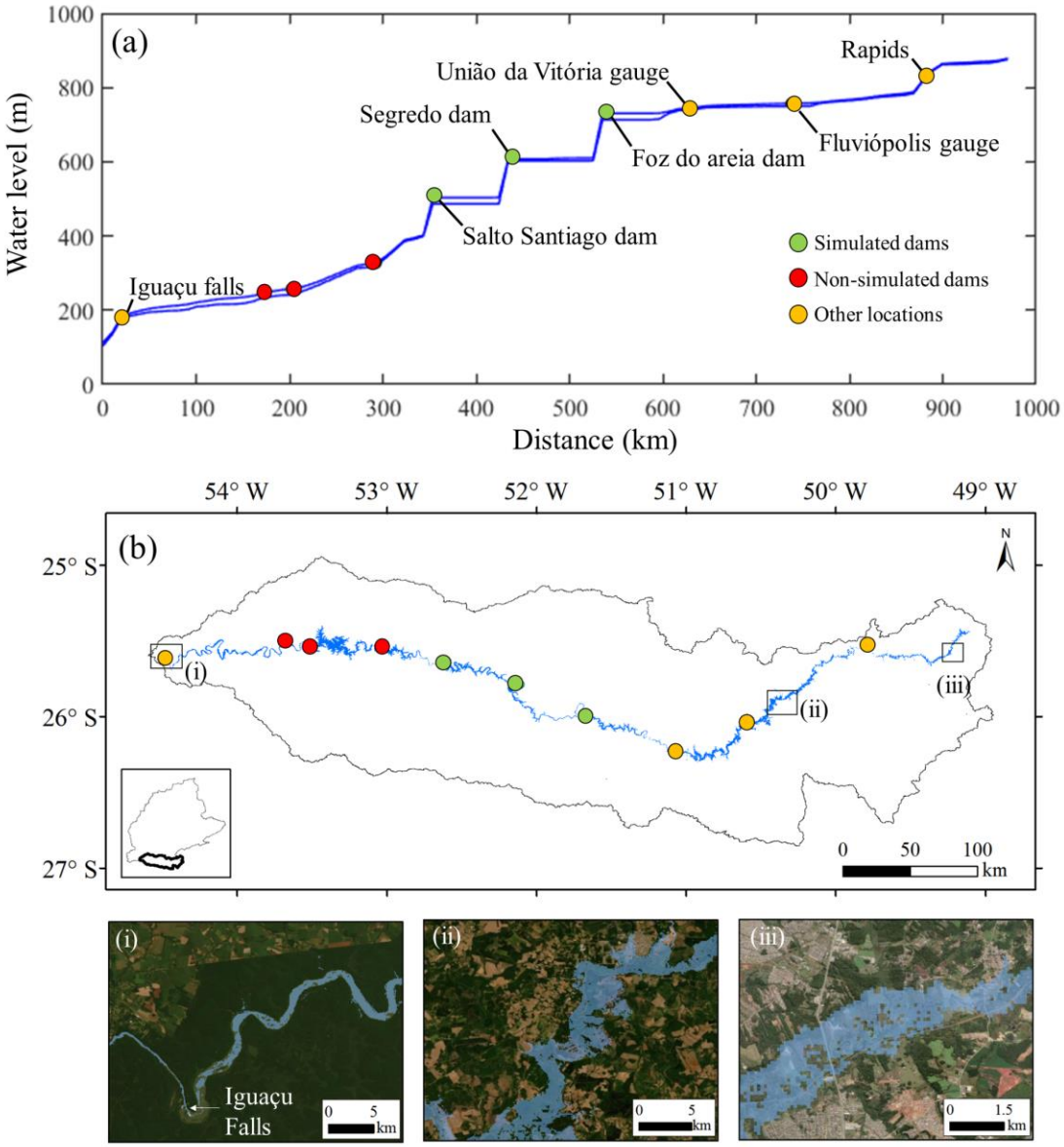

Figure 10. (a) Longitudinal profiles of maximum and minimum simulated surface water elevation (blue lines) along the Iguaçu river mainstem for the scenario REGVar. Distance is measured from the confluence between Iguaçu and Paraná rivers. The three regulation dams simulated along the Iguaçu mainstem are presented in the profile (green circles), as well as the run-of-river dams not simulated (red) and some locations of interest (yellow). (b) Maximum

807 simulated flood extent for the same reaches from figure a. Details (i), (ii) and (iii) show
808 particular areas together with Google Earth Imagery.

809

810 # 4 Discussion

811

812 ## 4.1 Improving the representation of reservoir operation in large scale models

813

814 This study compared generic reservoir operation schemes (H06 scenario, based
815 on Hanasaki et al. (2006)) to data-driven ones (scenarios 3PT, related to the three-point
816 rule curve, and REG, associated to linear regressions between monthly water levels and
817 dam outflows). As expected, the data-driven approach led to more accurate discharge
818 and storage estimates. For example, while the operation H06 outperformed 3PT in the
819 hydrology metrics, approaching REG, it provided the worst results in terms of tracking
820 observed storage (**Figure 7**). In this case, accumulated flow errors lead to poor storage
821 estimates (Turner et al., 2020). H06 has few parameters and it is apparently too simple
822 for a complex interconnected system. In turn, the REG scheme is similar to the one by
823 Solander et al. (2016) in the way that it fits a relation between storage and outflow. It is
824 also related to Yassin et al. (2019), since it estimates the actual operational levels from
825 observed data at a monthly basis, adopting dam characteristics for levels out of the
826 observed ranges, thus emulating the actual reservoir rule curve. The satisfactory
827 performance of this rule is also associated to relatively low bias in MGB estimates (see
828 Supplementary Material S1), since inflow bias can largely affect reservoir simulation
829 schemes (Turner et al., 2020).

830 The global-based parameterization (i.e., the one that does not require
831 regionally/locally available detailed data) led to a slightly poorer performance in

comparison to the regional-based one for discharge, and it was generally more accurate than naturalized flows, providing a reasonable approach to represent hydrological alteration at regional scales.

Finally, the results from the adopted operations should be analyzed by considering the context in which the real system is operated. In Brazil, the actual operation of all major dams is defined considering the large-scale interconnected hydrothermal power system (SIN), based on operational decisions reallocating storage inter-temporally throughout the system to minimize spills and energy production costs. The SIN is divided into regional interconnected subsystems (South, South-east, Central-west, Northeast and North) with significantly diverse hydrological characteristics. As the operation of a given hydropower plant affects others units downstream, a system wide operation strategy prevails over individual ones. First, an energy generation solution is determined for the whole system, which is later disaggregated to individual power units. Given the high contribution of hydropower in the mix (over 65%) and stochasticity of inflows, operating costs depend on present and future decisions. ONS defines the dispatch schedule for all generating units connected in the SIN (hydropower, thermal, wind and nuclear) on a monthly basis based on a merit order (from lower to higher cost), and considering current reservoir storage and flow forecasts. Hence, when a group of reservoirs is low in storage in a given region, hydropower plants from another region can be dispatched and the energy transferred, avoiding the use of local thermal plants. The coordinated operation ranges from long term (four years) to dispatch scheduling (every half hour).

The improvement of regional scale models may involve hedging operations (reducing releases to minimize the probability of more severe cutbacks in the future ; You & Cai (2008)) and coordinated operations (Marques & Tilmant, 2013; Marques et

al., 2006; Rougé et al., 2019), which are typically not considered. In this study, the REG scheme was designed to represent an average behavior (rule curve) of the coordinated system, which trades off its capability to depict anomalous years (especially dry ones). Approaches focusing on a single reservoir may disregard basin-scale flood or drought control that exists within a coordinated operation (Rougé et al., 2019). Furthermore, to improve estimates, a detailed operation would require the representation of actual hydraulic structures (spillways, outlet works, etc.) (Fleischmann et al., 2019a) which is not always available to dams worldwide. As our purpose is to perform regional scale simulations, simplified operations were chosen for better model applicability. Potential future improvements should expand the REG operation to multiple regressions including other relevant explanatory variables beyond observed levels (e.g., Solander et al. (2016)). These relevant variables should be chosen based on homogeneous behavior in specific regions (i.e. not all regions would have the same explanatory variables with the same coefficients). On the other hand, the proposed methodology could be easily expanded to continental scale domains (e.g., Siqueira et al. (2018)), provided information on dam characteristics as stage-area curves and observed time series of storage and outflows is available. Finally, the proposed operation approaches do not take into account water withdrawals and consumptive demands associated (e.g. irrigation), as those are small in the context of the studied Paraná basin, and their effect is localized, so that we focused on hydropower generation dams instead. In future work, distributed modeling systems should explicitly simulate reservoir dynamics, as more information becomes available. In Brazil, recent national scale mapping of irrigation schemes (ANA, 2017) could be coupled to the MGB framework, combined with recent developments in large scale modeling of reservoir operation under timely varying water

demands (Biemans et al., 2011; Haddeland et al., 2014; Hanasaki et al., 2006; Voisin et al., 2017).

4.2 On the importance of representing the river-floodplain-reservoir continuum in large scale models

The presented model of the river-floodplain-reservoir continuum at regional scale provides a continuous depiction of the spatial-temporal variation of hydraulic variables as water surface elevation and flood extent and storage. The consideration of a distributed reservoir bathymetry was shown to be fundamental to estimate backwater effects, as revealed by a basin-scale comparison between lumped and distributed schemes (equal and variable bathymetry), and an ICESat-based validation of the Itaipu reservoir longitudinal water level profile. Backwater effects are required for many applications, e.g., to perform real-time monitoring of the impact of a given reservoir on an upstream city (see the Iguaçu River case study in Section 3.3), or to correctly estimate the dam inflow along lateral tributaries.

A correct representation of hydrodynamics at the basin scale was also shown to be fundamental for flood frequency analysis, considering both reservoirs and floodplains' effects (Fleischmann et al., 2019a; Tanaka et al., 2017; Wang et al., 2017; Zajac et al., 2017; Zhao et al., 2020). Project flood discharges are usually estimated with simplified methods as unit hydrographs that do not consider river floodplain attenuation. An interesting and open research question relates to how far upstream can these floodplain storage effects go, what has major implications for water resources management. Floodplains alter the celerity of flood waves at the whole basin scale, and are a major driver of hydrograph shape across scales (Collischonn et al., 2017; Fleischmann et al.,

2016). Besides, here we have assessed the role of flood attenuation in riverine wetlands, while at the very upstream reaches, upland rain-fed wetlands may also change towards flood generating areas, requiring further studies (Acreman and Holden, 2013).

Natural floodplains provide valuable ecosystem services in terms of flood attenuation and resilience, and its quantification requires new tools (Ameli & Creed, 2019; Wu et al., 2020). Building new dams (especially if designed for purposes different than flood control), as well as new developments in floodplain areas (e.g., levees), may remove the large floodplain storage effects that protect downstream reaches against floods. This was shown for many rivers, as the Mississippi with hundreds of kilometers of levees deactivating the river natural flood storage (Hey and Philippi, 1995) and the Danube river (Schober et al., 2014). Furthermore, a benefit-cost analysis of acquiring floodplain lands to avoid flood damage was performed for the whole USA recently (Johnson et al., 2020), and suggested that the cumulative flood damages exceeds the costs of land acquisition for a 2070 scenario. The synergic effects of reservoirs and floodplains on flood attenuation have been increasingly addressed in the literature with large scale models (Shin et al., 2020), and are in accordance with our results. The analysis and modeling improvements provided here indicate that the synergy between floodable areas and the operation of dam cascades at the whole basin scale is relevant and requires further understanding, which is beyond simpler large scale models relying solely on hydrodynamic simulations along downstream floodable areas. In the case of the Paraná basin, inserting the proposed methodology into a proper flood risk management framework will require real-time flood monitoring and forecasting.

4.3 Perspectives on simulating the river-floodplain-reservoir continuum at large scales

The development of coupled river-floodplain-reservoir modeling systems is associated to the hyper-resolution global modeling agenda, aiming for example to improve medium-range flood forecasts (Zajac et al., 2017) that are locally relevant (Bierkens et al., 2015; Fleischmann et al., 2019c; Rajib et al., 2020; Wood et al., 2011) within land surface, earth system or global hydrological models, and explicitly representing reservoir dynamics within detailed grids (Shin et al., 2019; Wada et al., 2016; Zajac et al., 2017). From continental to global scales, these models are powerful tools to assist national and world agencies on the coordinated planning of reservoir expansion, as well as understanding the effects of current and future dams on water and biogeochemical cycles (Bierkens et al., 2015; Wada et al., 2016), and their interaction with climate change, contributing to improve global water security (Adam et al., 2007; Arias et al., 2020; Dang et al., 2019; Ehsani et al., 2017; Poff et al., 2016; Williamson et al., 2009). On the other hand, from local to regional scales, they can be used for actual dam operation, real-time monitoring and forecasting systems, and estimation of locally relevant discharges at high spatial-temporal resolution.

The necessity of spatially and temporally continuous fields of state variables as river discharges and levels has prompted the combination of remote sensing datasets and hydraulic models (Brêda et al., 2019; Gleason and Durand, 2020). ICESat altimetry data provide valuable information for lakes (Gao, 2015; O'Loughlin et al., 2016) and are very promising for validating large scale reservoir modeling systems, while new missions as ICESat-2 (threefold increase in sampling density) and SWOT will increase our capability to remotely monitor reservoirs and estimate reservoir parameters and

even reservoir operation (Bonnema & Hossain, 2017, 2019; Busker et al., 2019; Getirana et al., 2018; Van Den Hoek et al., 2019; Yao et al., 2019; Yoon et al., 2016; Yoon & Beighley, 2015). New global datasets of reservoir characteristics are also promising, including new methodologies to estimate reservoir area-depth-volume relationships based on remote-sensing datasets (Crétaux et al., 2016; Fassoni-Andrade et al., 2020; Gao et al., 2012; Lehner et al., 2011; Li et al., 2020; Liebe et al., 2005; Mulligan et al., 2020; Yigzaw et al., 2019, 2018). These advances contributed to the development of reservoir representation in global hydrological models (Döll et al., 2009; Sutanudjaja et al., 2018; Voisin et al., 2013; Wada et al., 2016; Yassin et al., 2019; Zhou et al., 2017), including the data-driven operations schemes as presented here and in other recent studies (Turner et al., 2020), and are shaping the new generation of large scale water resources models.

Regarding large scale model improvement, we have adopted a 10 km river reach discretization for the Paraná basin, in accordance with current practices adopted in regional to global hydrological models (i.e., 5-10 km; Shin et al., 2019; Wada et al., 2016; Zajac et al., 2017). However, higher resolution (i.e., 1 km or smaller) are required to better represent relatively small dams. Our results indicate the need for better representation of reservoir bathymetry distribution in order to correctly address local scale hydraulic processes as backwater effects, corroborating recent studies (Adam et al., 2007; Shin et al., 2019).

Finally, we have also discussed the role of fully coupling hydrological-hydrodynamic processes in a two-way scheme. The MGB model considers a dynamic surface water cover, and the associated changes in evapotranspiration/runoff generation, e.g., by alternating the soil/vegetation Penman-Monteith equation with the open water Penam evaporation scheme. Considering reservoir evaporation was also implemented

by other modeling systems (Adam et al., 2007; Mamede et al., 2018; Zhao et al., 2016). This consideration is particularly important during dry periods, and even more important for reservoirs in semi-arid regions (Bonnema et al., 2016; Celeste and Billib, 2010; Döll et al., 2009; Mamede et al., 2018). Besides a dynamic flood fraction cover, other reservoir processes at local scale should also be included, as reservoir sedimentation (Zhao et al., 2016) and ground seepage.

5 Conclusions

In this study we presented the successful development and a thorough analysis of a regional scale model capable to simulate the daily river-floodplain-reservoir continuum that exists along large basins. A case study was performed in the ~950,000 km² Upper Paraná River Basin in South America, considering 30 regulation reservoirs and the Itaipu run-of-river dam, which is the largest in world in terms of energy production. Twelve simulation scenarios considering different reservoir bathymetry representation and reservoir operation schemes were performed, and assessed in terms of water levels, discharges, flood extent and reservoir storage. A methodology to assess the relative role of floodplains and reservoirs on basin-wide flood attenuation was presented, providing a powerful way to understand regional scale floods and the value of preserving natural floodplains' services. We conclude that:

- A distributed representation of reservoir bathymetry in large scale hydrological models is required for accurate predictions of backwater effects, upstream surface water elevation and flooding;

- Both lumped and distributed representations of reservoir bathymetry in large scale hydrological-hydrodynamic models provide similar predictions of downstream river discharges and water levels;

- A data-driven operation scheme based on historical data of reservoir storage and outflows adds significant value to the accuracy of reservoir storage predictions, if compared to more generic algorithms;

- Although the data-driven approach outperforms more generic schemes (namely, the H06 method) in terms of discharge estimation, the simpler generic schemes provide reasonable estimates, and thus can be useful to estimate regional scale hydrological regime alteration;

- Global-based parameterizations of operation schemes lead to only slightly poorer performance in comparison to more regionally-based ones, providing reasonable estimates of regional scale hydrological regime alteration;

- However, to properly simulate the river-floodplain-reservoir continuum at regional scale, satisfactory simulation of water levels and reservoir storages are required, and thus large-scale models should include data-driven reservoir operation approaches based on regional parameterization, and distributed reservoir bathymetry (if possible, with a variable bathymetry scheme);

- In the Paraná River Basin, the floodplains are mainly located in upper parts of some tributaries and in the river mainstem, while reservoir effects are more important for flood attenuation along medium and lower reaches of tributaries. In this case, floodplains and reservoirs provide complementary flood attenuation at regional scale;

- The existence of river floodplains across the whole basin can lead to major flood attenuation at the regional scale, and not only in downstream lowland reaches, as usually assumed in large scale models;
- Major overestimation of flood design discharges can occur if the model does not consider upstream floodplain and reservoir storage effects, especially in the context of flood frequency analysis.

Finally, our results stress the importance of simulating the river-floodplain-reservoir continuum at large scales. Increasing computational capacity with intense cloud computing, and new remote sensing-based datasets and techniques, are quickly pushing the development of large to global scale models, and thus improving to a great extent our understanding and prediction capability regarding reservoir-floodplain interactions.

Acknowledgments

This work was supported by CNPq (Conselho Nacional de Desenvolvimento Científico e Tecnológico, Brazil) [grant numbers 141161/2017-5 and 201148/2019-6]. We thank two anonymous reviewers for insightful contributions to our study.

References

Acreman, M., Holden, J., 2013. How wetlands affect floods. Wetlands 33, 773–786. https://doi.org/10.1007/s13157-013-0473-2

Adam, J.C., Haddeland, I., Su, F., Lettenmaier, D.P., 2007. Simulation of reservoir influences on annual and seasonal streamflow changes for the Lena, Yenisei, and Ob' rivers. J. Geophys. Res. 112, D24114. https://doi.org/10.1029/2007JD008525

Agostinho, A., Gomes, L.C., Zalewski, M., 2001. The importance of floodplains for the dynamics of fish communities of the upper river Paraná. Int. J. Ecohydrol. Hydrobiol. 1, 209–217.

Agostinho, A., Pelicice, F., Gomes, L., 2008. Dams and the fish fauna of the Neotropical region: impacts and management related to diversity and fisheries. Brazilian J. Biol. 68, 1119–1132. https://doi.org/10.1590/S1519-69842008000500019

Agostinho, A., Thomaz, S.M., Minte-Vera, C.V., Winemiller, K.O., 2000. Biodiversity in the High Parana River Floodplain.

Almeida, R.M., Shi, Q., Gomes-Selman, J.M., Wu, X., Xue, Y., Angarita, H., Barros, N., Forsberg, B.R., García-Villacorta, R., Hamilton, S.K., Melack, J.M., Montoya, M., Perez, G., Sethi, S.A., Gomes, C.P., Flecker, A.S., 2019. Reducing greenhouse gas emissions of Amazon hydropower with strategic dam planning. Nat. Commun. 10, 4281. https://doi.org/10.1038/s41467-019-12179-5

Ameli, A.A., Creed, I.F., 2019. Does Wetland Location Matter When Managing Wetlands for Watershed-Scale Flood and Drought Resilience? JAWRA J. Am. Water Resour. Assoc. 55, 529–542. https://doi.org/10.1111/1752-1688.12737

ANA, 2017. Atlas Irrigação: Uso da Água na Agricultura Irrigada. Brasília.

ANEEL, 2020. Sistema de Informações Geográficas do Setor Elétrico - SIGEL [WWW Document]. URL https://sigel.aneel.gov.br/portal/home/

Arias, M.E., Farinosi, F., Lee, E., Livino, A., Briscoe, J., Moorcroft, P.R., 2020. Impacts of climate change and deforestation on hydropower planning in the Brazilian Amazon. Nat. Sustain. https://doi.org/10.1038/s41893-020-0492-y

Bates, P.D., Horritt, M.S., Fewtrell, T.J., 2010. A simple inertial formulation of the shallow water equations for efficient two-dimensional flood inundation modelling. J. Hydrol. https://doi.org/10.1016/j.jhydrol.2010.03.027

Bates, P.D., Neal, J., Sampson, C., Smith, A., Trigg, M., 2018. Progress Toward Hyperresolution Models of Global Flood Hazard, in: Risk Modeling for Hazards and Disasters. Elsevier, pp. 211–232. https://doi.org/10.1016/B978-0-12-804071-3.00009-4

Baumgartner, M.T., de Oliveira, A.G., Agostinho, A.A., Gomes, L.C., 2018. Fish functional diversity responses following flood pulses in the upper Paraná River floodplain. Ecol. Freshw. Fish 27, 910–919. https://doi.org/10.1111/eff.12402

Biemans, H., Haddeland, I., Kabat, P., Ludwig, F., Hutjes, R.W.A., Heinke, J., Von Bloh, W., Gerten, D., 2011. Impact of reservoirs on river discharge and irrigation water supply during the 20th century. Water Resour. Res. 47, 1–15. https://doi.org/10.1029/2009WR008929

Bierkens, M.F.P., Bell, V.A., Burek, P., Chaney, N., Condon, L.E., David, C.H., de Roo, A., Döll, P., Drost, N., Famiglietti, J.S., Flörke, M., Gochis, D.J., Houser, P., Hut, R., Keune, J., Kollet, S., Maxwell, R.M., Reager, J.T., Samaniego, L., Sudicky, E., Sutanudjaja, E.H., van de Giesen, N., Winsemius, H., Wood, E.F., 2015. Hyper-resolution global hydrological modelling: What is next?: "Everywhere and locally relevant" M. F. P. Bierkens et al. Invited Commentary. Hydrol. Process. 29, 310–320. https://doi.org/10.1002/hyp.10391

Bonnema, M., Hossain, F., 2019. Assessing the Potential of the Surface Water and Ocean Topography Mission for Reservoir Monitoring in the Mekong River Basin. Water Resour. Res. 55, 444–461. https://doi.org/10.1029/2018WR023743

Bonnema, M., Hossain, F., 2017. Inferring reservoir operating patterns across the Mekong Basin using only space observations. Water Resour. Res. 53, 3791–3810. https://doi.org/10.1002/2016WR019978

Bonnema, M., Sikder, S., Miao, Y., Chen, X., Hossain, F., Ara Pervin, I., Mahbubur Rahman, S.M., Lee, H., 2016. Understanding satellite-based monthly-to-seasonal reservoir outflow estimation as a function of hydrologic controls. Water Resour. Res. 52, 4095–4115. https://doi.org/10.1002/2015WR017830

Boulanger, J.P., Leloup, J., Penalba, O., Rusticucci, M., Lafon, F., Vargas, W., 2005. Observed precipitation in the Paraná-Plata hydrological basin: Long-term trends, extreme conditions and ENSO teleconnections. Clim. Dyn. 24, 393–413. https://doi.org/10.1007/s00382-004-0514-x

Brêda, J.P.L.F., Paiva, R.C.D., Bravo, J.M., Passaia, O.A., Moreira, D.M., 2019. Assimilation of Satellite Altimetry Data for Effective River Bathymetry. Water Resour. Res. https://doi.org/10.1029/2018wr024010

Bueno, E. de O., Mello, C.R. de, Alves, G.J., 2016. Evaporation from Camargos hydropower plant reservoir: water footprint characterization. RBRH 21, 570–575. https://doi.org/10.1590/2318-0331.011616021

Busker, T., De Roo, A., Gelati, E., Schwatke, C., Adamovic, M., Bisselink, B., Pekel, J.F., Cottam, A., 2019. A global lake and reservoir volume analysis using a surface water dataset and satellite altimetry. Hydrol. Earth Syst. Sci. https://doi.org/10.5194/hess-23-669-2019

Celeste, A.B., Billib, M., 2010. The Role of Spill and Evaporation in Reservoir Optimization Models. Water Resour. Manag. 24, 617–628. https://doi.org/10.1007/s11269-009-9468-4

Collischonn, W., Allasia, D., da Silva, B.C., Tucci, C.E.M., 2007. The MGB-IPH model for large-scale rainfall-runoff modelling. Hydrol. Sci. J. https://doi.org/10.1623/hysj.52.5.878

Collischonn, W., Fleischmann, A., Paiva, R.C.D., Mejia, A., 2017. Hydraulic Causes for Basin Hydrograph Skewness. Water Resour. Res. 53, 10603–10618. https://doi.org/10.1002/2017WR021543

Crétaux, J.F., Abarca-del-Río, R., Berge-Nguyen, M., Arsen, A., Drolon, V., Clos, G., Maisongrande, P., 2016. Lake Volume Monitoring from Space. Surv. Geophys. 37, 269–305. https://doi.org/10.1007/s10712-016-9362-6

Dang, T.D., Chowdhury, A.K., Galelli, S., 2019. On the representation of water reservoir storage and operations in large-scale hydrological models: implications on model parameterization and climate change impact assessments. Hydrol. Earth Syst. Sci. Discuss. 1–34. https://doi.org/10.5194/hess-2019-334

Degu, A.M., Hossain, F., Niyogi, D., Pielke, R., Shepherd, J.M., Voisin, N., Chronis, T., 2011. The influence of large dams on surrounding climate and precipitation patterns. Geophys. Res. Lett. 38, n/a-n/a. https://doi.org/10.1029/2010GL046482

Di Baldassarre, G., Kooy, M., Kemerink, J.S., Brandimarte, L., 2013. Towards understanding the dynamic behaviour of floodplains as human-water systems. Hydrol. Earth Syst. Sci. 17, 3235–3244. https://doi.org/10.5194/hess-17-3235-2013

Döll, P., Fiedler, K., Zhang, J., 2009. Global-scale analysis of river flow alterations due to water withdrawals and reservoirs. Hydrol. Earth Syst. Sci. 13, 2413–2432. https://doi.org/10.5194/hess-13-2413-2009

Doyle, M.E., Barros, V.R., 2011. Attribution of the river flow growth in the Plata Basin.

Int. J. Climatol. 31, 2234–2248. https://doi.org/10.1002/joc.2228

Draper, A.J., Lund, J.R., 2004. Optimal Hedging and Carryover Storage Value. J. Water Resour. Plan. Manag. 130, 83–87. https://doi.org/10.1061/(ASCE)0733-9496(2004)130:1(83)

Droppers, B., Franssen, W.H.P., van Vliet, M.T.H., Nijssen, B., Ludwig, F., 2020. Simulating human impacts on global water resources using VIC-5. Geosci. Model Dev. 13, 5029–5052. https://doi.org/10.5194/gmd-13-5029-2020

Ehsani, N., Vörösmarty, C.J., Fekete, B.M., Stakhiv, E.Z., 2017. Reservoir operations under climate change: Storage capacity options to mitigate risk. J. Hydrol. 555, 435–446. https://doi.org/10.1016/j.jhydrol.2017.09.008

Fan, F., Buarque, D.C., Pontes, P.R.M., Collischonn, W., 2015. Um mapa de unidades de resposta hidrológica para a América do Sul., in: Anais Do XXI Simpósio Brasileiro de Recursos Hídricos. ABRH, Brasília, p. PAP019919.

Fassoni-Andrade, A.C., de Paiva, R.C.D., Fleischmann, A.S., 2020. Lake Topography and Active Storage From Satellite Observations of Flood Frequency. Water Resour. Res. https://doi.org/10.1029/2019WR026362

Fleischmann, A., Collischonn, W., Paiva, R., Tucci, C.E., 2019a. Modeling the role of reservoirs versus floodplains on large-scale river hydrodynamics. Nat. Hazards 99, 1075–1104. https://doi.org/10.1007/s11069-019-03797-9

Fleischmann, A., Fan, F., Collischonn, B., Collischonn, W., Pontes, P., Ruhoff, A., 2019b. Precipitation as a proxy for climate variables: application for hydrological modelling. Hydrol. Sci. J. 64, 361–379. https://doi.org/10.1080/02626667.2019.1587169

Fleischmann, A., Paiva, R., Collischonn, W., 2019c. Can regional to continental river hydrodynamic models be locally relevant? A cross-scale comparison. J. Hydrol. X 3, 100027. https://doi.org/10.1016/j.hydroa.2019.100027

Fleischmann, A.S., Paiva, R.C.D., Collischonn, W., Siqueira, V.A., Paris, A., Moreira, D.M., Papa, F., Bitar, A.A., Parrens, M., Aires, F., Garambois, P.A., 2020. Trade-Offs Between 1-D and 2-D Regional River Hydrodynamic Models. Water Resour. Res. 56. https://doi.org/10.1029/2019WR026812

Fleischmann, A.S., Paiva, R.C.D., Collischonn, W., Sorribas, M. V., Pontes, P.R.M., 2016. On river-floodplain interaction and hydrograph skewness. Water Resour. Res. 52, 7615–7630. https://doi.org/10.1002/2016WR019233

Fread, D., 1992. Flow routing, in: Maidment, D.R. (Ed.), Handbook of Hydrology.

Gao, H., 2015. Satellite remote sensing of large lakes and reservoirs: from elevation and area to storage. Wiley Interdiscip. Rev. Water 2, 147–157. https://doi.org/10.1002/wat2.1065

Gao, H., Birkett, C., Lettenmaier, D.P., 2012. Global monitoring of large reservoir storage from satellite remote sensing. Water Resour. Res. 48, 1–12. https://doi.org/10.1029/2012WR012063

Getirana, A., Jung, H.C., Tseng, K.H., 2018. Deriving three dimensional reservoir bathymetry from multi-satellite datasets. Remote Sens. Environ. 217, 366–374. https://doi.org/10.1016/j.rse.2018.08.030

Getirana, A., Peters-Lidard, C., Rodell, M., Bates, P.D., 2017. Trade-off between cost and accuracy in large-scale surface water dynamic modeling. Water Resour. Res. 53, 4942–4955. https://doi.org/10.1002/2017WR020519

1188 Gleason, C.J., Durand, M.T., 2020. Remote Sensing of River Discharge : A Review and
1189 a Framing for the Discipline 2, 1–28.

1190 Grill, G., Lehner, B., Thieme, M., Geenen, B., Tickner, D., Antonelli, F., Babu, S.,
1191 Borrelli, P., Cheng, L., Crochetiere, H., Ehalt Macedo, H., Filgueiras, R., Goichot,
1192 M., Higgins, J., Hogan, Z., Lip, B., McClain, M.E., Meng, J., Mulligan, M.,
1193 Nilsson, C., Olden, J.D., Opperman, J.J., Petry, P., Reidy Liermann, C., Sáenz, L.,
1194 Salinas-Rodríguez, S., Schelle, P., Schmitt, R.J.P., Snider, J., Tan, F., Tockner, K.,
1195 Valdujo, P.H., van Soesbergen, A., Zarfl, C., 2019. Mapping the world's free-
1196 flowing rivers. Nature 569, 215–221. https://doi.org/10.1038/s41586-019-1111-9

1197 Haddeland, I., Heinke, J., Biemans, H., Eisner, S., Flörke, M., Hanasaki, N., Konzmann,
1198 M., Ludwig, F., Masaki, Y., Schewe, J., Stacke, T., Tessler, Z.D., Wada, Y.,
1199 Wisser, D., 2014. Global water resources affected by human interventions and
1200 climate change. Proc. Natl. Acad. Sci. U. S. A. 111, 3251–3256.
1201 https://doi.org/10.1073/pnas.1222475110

1202 Haddeland, I., Skaugen, T., Lettenmaier, D.P., 2006. Anthropogenic impacts on
1203 continental surface water fluxes. Geophys. Res. Lett. 33, 2–5.
1204 https://doi.org/10.1029/2006GL026047

1205 Hanasaki, N., Kanae, S., Oki, T., 2006. A reservoir operation scheme for global river
1206 routing models. J. Hydrol. 327, 22–41.
1207 https://doi.org/10.1016/j.jhydrol.2005.11.011

1208 Hanasaki, N., Yoshikawa, S., Pokhrel, Y., Kanae, S., 2018. A global hydrological
1209 simulation to specify the sources of water used by humans. Hydrol. Earth Syst. Sci.
1210 22, 789–817. https://doi.org/10.5194/hess-22-789-2018

1211 Hey, D.L., Philippi, N.S., 1995. Flood Reduction through Wetland Restoration: The

Upper Mississippi River Basin as a Case History. Restor. Ecol. 3, 4–17. https://doi.org/10.1111/j.1526-100X.1995.tb00070.x

Ho, M., Lall, U., Allaire, M., Devineni, N., Kwon, H.H., Pal, I., Raff, D., Wegner, D., 2017. The future role of dams in the United States of America. Water Resour. Res. 53, 982–998. https://doi.org/10.1002/2016WR019905

Hossain, F., Degu, A.M., Yigzaw, W., Burian, S., Niyogi, D., Shepherd, J.M., Pielke, R., 2012. Climate Feedback–Based Provisions for Dam Design, Operations, and Water Management in the 21st Century. J. Hydrol. Eng. 17, 837–850. https://doi.org/10.1061/(ASCE)HE.1943-5584.0000541

Itaipu, 2016. RELATÓRIO ANUAL ITAIPU BINACIONAL.

Jardini, J.A., Ramos, D.S., Martini, J.S.C., Reis, L.B., Tahan, C.M.A., 2002. Brazilian Energy Crisis. IEEE Power Eng. Rev. 22, 21–24. https://doi.org/10.1109/MPER.2002.994845

Johnson, K.A., Wing, O.E.J., Bates, P.D., Fargione, J., Kroeger, T., Larson, W.D., Sampson, C.C., Smith, A.M., 2020. A benefit–cost analysis of floodplain land acquisition for US flood damage reduction. Nat. Sustain. 3, 56–62. https://doi.org/10.1038/s41893-019-0437-5

L. Gutenson, J., A. Tavakoly, A., D. Wahl, M., L. Follum, M., 2020. Comparison of generalized non-data-driven lake and reservoir routing models for global-scale hydrologic forecasting of reservoir outflow at diurnal time steps. Hydrol. Earth Syst. Sci. 24, 2711–2729. https://doi.org/10.5194/hess-24-2711-2020

Lee, E., Livino, A., Han, S.C., Zhang, K., Briscoe, J., Kelman, J., Moorcroft, P., 2018. Land cover change explains the increasing discharge of the Paraná River. Reg.

Environ. Chang. 18, 1871–1881. https://doi.org/10.1007/s10113-018-1321-y

Lehner, B., Liermann, C.R., Revenga, C., Vörömsmarty, C., Fekete, B., Crouzet, P., Döll, P., Endejan, M., Frenken, K., Magome, J., Nilsson, C., Robertson, J.C., Rödel, R., Sindorf, N., Wisser, D., 2011. High-resolution mapping of the world's reservoirs and dams for sustainable river-flow management. Front. Ecol. Environ. 9, 494–502. https://doi.org/10.1890/100125

Lehner, B., Verdin, K., Jarvis, A., 2008. New global hydrography derived from spaceborne elevation data. Eos (Washington. DC). https://doi.org/10.1029/2008EO100001

Li, Y., Gao, H., Zhao, G., Tseng, K.H., 2020. A high-resolution bathymetry dataset for global reservoirs using multi-source satellite imagery and altimetry. Remote Sens. Environ. 244, 111831. https://doi.org/10.1016/j.rse.2020.111831

Liebe, J., van de Giesen, N., Andreini, M., 2005. Estimation of small reservoir storage capacities in a semi-arid environment. Phys. Chem. Earth. https://doi.org/10.1016/j.pce.2005.06.011

Mamede, G.L., Guentner, A., Medeiros, P.H.A., de Araújo, J.C., Bronstert, A., 2018. Modeling the Effect of Multiple Reservoirs on Water and Sediment Dynamics in a Semiarid Catchment in Brazil. J. Hydrol. Eng. 23, 05018020. https://doi.org/10.1061/(ASCE)HE.1943-5584.0001701

Marques, G.F., Tilmant, A., 2013. The economic value of coordination in large-scale multireservoir systems: The Parana River case. Water Resour. Res. 49, 7546–7557. https://doi.org/10.1002/2013WR013679

Marques, T.C., Cicogna, M.A., Soares, S., 2006. Benefits of coordination in the

operation of hydroelectric power systems: Brazilian case, in: 2006 IEEE Power Engineering Society General Meeting. IEEE, p. 8 pp. https://doi.org/10.1109/PES.2006.1709574

Mateo, C.M., Hanasaki, N., Komori, D., Tanaka, K., Kiguchi, M., Champathong, A., Sukhapunnaphan, T., Yamazaki, D., Oki, T., 2014. Assessing the impacts of reservoir operation to floodplain inundation by combining hydrological, reservoir management, and hydrodynamic models. Water Resour. Res. 50, 7245–7266. https://doi.org/10.1002/2013WR014845

Minotti, P.G., 2018. The Paraná-Paraguay Fluvial Corridor (Argentina), in: The Wetland Book. Springer Netherlands, Dordrecht, pp. 785–796. https://doi.org/10.1007/978-94-007-4001-3_242

Mulligan, M., van Soesbergen, A., Sáenz, L., 2020. GOODD, a global dataset of more than 38,000 georeferenced dams. Sci. Data. https://doi.org/10.1038/s41597-020-0362-5

Nazemi, A., Wheater, H.S., 2015. On inclusion of water resource management in Earth system models - Part 2: Representation of water supply and allocation and opportunities for improved modeling. Hydrol. Earth Syst. Sci. 19, 63–90. https://doi.org/10.5194/hess-19-63-2015

Neal, J., Schumann, G., Bates, P., 2012. A subgrid channel model for simulating river hydraulics and floodplain inundation over large and data sparse areas. Water Resour. Res. 48, 1–16. https://doi.org/10.1029/2012WR012514

Nilsson, C., 2005. Fragmentation and Flow Regulation of the World's Large River Systems. Science (80-.). 308, 405–408. https://doi.org/10.1126/science.1107887

O'Loughlin, F.E., Neal, J., Yamazaki, D., Bates, P.D., 2016. ICESat-derived inland water surface spot heights. Water Resour. Res. 52, 3276–3284. https://doi.org/10.1002/2015WR018237

Oliveira, R., Loucks, D.P., 1997. Operating rules for multireservoir systems. Water Resour. Res. 33, 839–852. https://doi.org/10.1029/96WR03745

ONS, 2020. Diagrama Esquemático das Usinas Hidroelétricas do SIN [WWW Document]. URL http://www.ons.org.br/

ONS, 2019. Manual de procedimentos da operação 10.2.1. Rio de Janeiro.

Paiva, R., Buarque, D.C., Collischonn, W., Bonnet, M.P., Frappart, F., Calmant, S., Bulhões Mendes, C.A., 2013. Large-scale hydrologic and hydrodynamic modeling of the Amazon River basin. Water Resour. Res. 49, 1226–1243. https://doi.org/10.1002/wrcr.20067

Paiva, R.C.D., Collischonn, W., Tucci, C.E.M., 2011. Large scale hydrologic and hydrodynamic modeling using limited data and a GIS based approach. J. Hydrol. 406, 170–181. https://doi.org/10.1016/j.jhydrol.2011.06.007

Pande, S., Sivapalan, M., 2017. Progress in socio-hydrology: a meta-analysis of challenges and opportunities. Wiley Interdiscip. Rev. Water 4, e1193. https://doi.org/10.1002/wat2.1193

Poff, N.L., Brown, C.M., Grantham, T.E., Matthews, J.H., Palmer, M.A., Spence, C.M., Wilby, R.L., Haasnoot, M., Mendoza, G.F., Dominique, K.C., Baeza, A., 2016. Sustainable water management under future uncertainty with eco-engineering decision scaling. Nat. Clim. Chang. 6, 25–34. https://doi.org/10.1038/nclimate2765

Poff, N.L., Richter, B.D., Arthington, A.H., Bunn, S.E., Naiman, R.J., Kendy, E.,

Acreman, M., Apse, C., Bledsoe, B.P., Freeman, M.C., Henriksen, J., Jacobson, R.B., Kennen, J.G., Merritt, D.M., O'Keeffe, J.H., Olden, J.D., Rogers, K., Tharme, R.E., Warner, A., 2010. The ecological limits of hydrologic alteration (ELOHA): A new framework for developing regional environmental flow standards. Freshw. Biol. 55, 147–170. https://doi.org/10.1111/j.1365-2427.2009.02204.x

Pokhrel, Y., Hanasaki, N., Koirala, S., Cho, J., Yeh, P.J.F., Kim, H., Kanae, S., Oki, T., 2012. Incorporating Anthropogenic Water Regulation Modules into a Land Surface Model. J. Hydrometeorol. 13, 255–269. https://doi.org/10.1175/JHM-D-11-013.1

Pokhrel, Y., Shin, S., Lin, Z., Yamazaki, D., Qi, J., 2018. Potential Disruption of Flood Dynamics in the Lower Mekong River Basin Due to Upstream Flow Regulation. Sci. Rep. 8, 17767. https://doi.org/10.1038/s41598-018-35823-4

Pokhrel, Y.N., Hanasaki, N., Wada, Y., Kim, H., 2016. Recent progresses in incorporating human land-water management into global land surface models toward their integration into Earth system models. Wiley Interdiscip. Rev. Water 3, 548–574. https://doi.org/10.1002/wat2.1150

Pontes, P.R.M., Fan, F.M., Fleischmann, A.S., de Paiva, R.C.D., Buarque, D.C., Siqueira, V.A., Jardim, P.F., Sorribas, M.V., Collischonn, W., 2017. MGB-IPH model for hydrological and hydraulic simulation of large floodplain river systems coupled with open source GIS. Environ. Model. Softw. 94, 1–20. https://doi.org/10.1016/j.envsoft.2017.03.029

Rajib, A., Liu, Z., Merwade, V., Tavakoly, A.A., Follum, M.L., 2020. Towards a large-scale locally relevant flood inundation modeling framework using SWAT and LISFLOOD-FP. J. Hydrol. 581, 124406.

https://doi.org/10.1016/j.jhydrol.2019.124406

Rennó, C.D., Nobre, A.D., Cuartas, L.A., Soares, J.V., Hodnett, M.G., Tomasella, J., Waterloo, M.J., 2008. HAND, a new terrain descriptor using SRTM-DEM: Mapping terra-firme rainforest environments in Amazonia. Remote Sens. Environ. https://doi.org/10.1016/j.rse.2008.03.018

Richter, B.D., Thomas, G.A., 2007. Restoring environmental flows by modifying dam operations. Ecol. Soc. https://doi.org/10.5751/ES-02014-120112

Rougé, C., Reed, P., Grogan, D., Zuidema, S., Prusevich, A., Glidden, S., Lamontagne, J., Lammers, R., 2019. Coordination and Control: Limits in Standard Representations of Multi-Reservoir Operations in Hydrological Modeling. Hydrol. Earth Syst. Sci. Discuss. 1–37. https://doi.org/10.5194/hess-2019-589

Santos, C.P., 2015. Efeitos da cascata de reservatórios sobre a variabilidade natural de vazões : o caso do rio Paraná em Porto Primavera 20, 698–707. https://doi.org/10.21168/rbrh.v20n3.p698-707

Schmitt Quedi, E., Mainardi Fan, F., 2020. Sub seasonal streamflow forecast assessment at large-scale basins. J. Hydrol. https://doi.org/10.1016/j.jhydrol.2020.124635

Schmitt, R.J.P., Bizzi, S., Castelletti, A., Opperman, J.J., Kondolf, G.M., 2019. Planning dam portfolios for low sediment trapping shows limits for sustainable hydropower in the Mekong. Sci. Adv. 5, eaaw2175. https://doi.org/10.1126/sciadv.aaw2175

Schober, B., Hauer, C., Habersack, H., 2014. A novel assessment of the role of Danube floodplains in flood hazard reduction (FEM method). Nat. Hazards 75, 33–50. https://doi.org/10.1007/s11069-013-0880-y

Schumann, J.-P., Neal, J.C., Voisin, N., Andreadis, K.M., Pappenberger, F., Phanthuwongpakdee, N., Hall, A.C., Bates, P.D., Schumann, C.:, 2013. A first large scale flood inundation forecasting model. Water Resour. Res 49, 6248–6257. https://doi.org/10.1002/wrcr.20521

Schutz, B.E., Zwally, H.J., Shuman, C.A., Hancock, D., DiMarzio, J.P., 2005. Overview of the ICESat mission. Geophys. Res. Lett. https://doi.org/10.1029/2005GL024009

Semertzidis, T., Spataru, C., Bleischwitz, R., 2019. The Nexus: Estimation of Water Consumption for Hydropower in Brazil. J. Sustain. Dev. Energy, Water Environ. Syst. 7, 122–138. https://doi.org/10.13044/j.sdewes.d6.0229

Shin, S., Pokhrel, Y., Miguez-Macho, G., 2019. High-Resolution Modeling of Reservoir Release and Storage Dynamics at the Continental Scale. Water Resour. Res. 55, 787–810. https://doi.org/10.1029/2018WR023025

Shin, S., Pokhrel, Y., Yamazaki, D., Huang, X., Torbick, N., Qi, J., Pattanakiat, S., Ngo-Duc, T., Nguyen, T.D., 2020. High Resolution Modeling of River-Floodplain-Reservoir Inundation Dynamics in the Mekong River Basin. Water Resour. Res. 56. https://doi.org/10.1029/2019WR026449

Siqueira, V., Fleischmann, A., Jardim, P., Fan, F., Collischonn, W., 2016. IPH-Hydro Tools: uma ferramenta open source para determinação de informações topológicas em bacias hidrográficas integrada a um ambiente SIG. Rev. Bras. Recur. Hídricos 21, 274–287. https://doi.org/10.21168/rbrh.v21n1.p274-287

Siqueira, V.A., Paiva, R.C.D., Fleischmann, A.S., Fan, F.M., Ruhoff, A.L., Pontes, P.R.M., Paris, A., Calmant, S., Collischonn, W., 2018. Toward continental hydrologic–hydrodynamic modeling in South America. Hydrol. Earth Syst. Sci. 22, 4815–4842. https://doi.org/10.5194/hess-22-4815-2018

Solander, K.C., Reager, J.T., Thomas, B.F., David, C.H., Famiglietti, J.S., 2016. Simulating human water regulation: The development of an optimal complexity, climate-adaptive reservoir management model for an LSM. J. Hydrometeorol. 17, 725–744. https://doi.org/10.1175/JHM-D-15-0056.1

Sutanudjaja, E.H., van Beek, R., Wanders, N., Wada, Y., Bosmans, J.H.C., Drost, N., van der Ent, R.J., de Graaf, I.E.M., Hoch, J.M., de Jong, K., Karssenberg, D., López López, P., Peßenteiner, S., Schmitz, O., Straatsma, M.W., Vannametee, E., Wisser, D., Bierkens, M.F.P., 2018. PCR-GLOBWB 2: a 5arcmin global hydrological and water resources model. Geosci. Model Dev. 11, 2429–2453. https://doi.org/10.5194/gmd-11-2429-2018

Tanaka, T., Tachikawa, Y., Iachikawa, Y., Yorozu, K., 2017. Impact assessment of upstream flooding on extreme flood frequency analysis by incorporating a flood-inundation model for flood risk assessment. J. Hydrol. 554, 370–382. https://doi.org/10.1016/j.jhydrol.2017.09.012

Trigg, M.A., Birch, C.E., Neal, J.C., Bates, P.D., Smith, A., Sampson, C.C., Yamazaki, D., Hirabayashi, Y., Pappenberger, F., Dutra, E., Ward, P.J., Winsemius, H.C., Salamon, P., Dottori, F., Rudari, R., Kappes, M.S., Simpson, A.L., Hadzilacos, G., Fewtrell, T.J., 2016. The credibility challenge for global fluvial flood risk analysis. Environ. Res. Lett. 11, 094014. https://doi.org/10.1088/1748-9326/11/9/094014

Trigg, M.A., Wilson, M.D., Bates, P.D., Horritt, M.S., Alsdorf, D.E., Forsberg, B.R., Vega, M.C., 2009. Amazon flood wave hydraulics. J. Hydrol. 374, 92–105. https://doi.org/10.1016/j.jhydrol.2009.06.004

Turner, S.W.D., Doering, K., Voisin, N., 2020. Data-Driven Reservoir Simulation in a Large-Scale Hydrological and Water Resource Model. Water Resour. Res. 56.

https://doi.org/10.1029/2020wr027902

van Beek, L.P.H., Wada, Y., Bierkens, M.F.P., 2011. Global monthly water stress: 1. Water balance and water availability. Water Resour. Res. 47. https://doi.org/10.1029/2010WR009791

Van Den Hoek, J., Getirana, A., Jung, H., Okeowo, M., Lee, H., 2019. Monitoring Reservoir Drought Dynamics with Landsat and Radar/Lidar Altimetry Time Series in Persistently Cloudy Eastern Brazil. Remote Sens. 11, 827. https://doi.org/10.3390/rs11070827

Viglione, A., Di Baldassarre, G., Brandimarte, L., Kuil, L., Carr, G., Salinas, J.L., Scolobig, A., Blöschl, G., 2014. Insights from socio-hydrology modelling on dealing with flood risk – Roles of collective memory, risk-taking attitude and trust. J. Hydrol. 518, 71–82. https://doi.org/10.1016/j.jhydrol.2014.01.018

Voisin, N., Hejazi, M.I., Leung, L.R., Liu, L., Huang, M., Li, H.-Y., Tesfa, T., 2017. Effects of spatially distributed sectoral water management on the redistribution of water resources in an integrated water model. Water Resour. Res. 53, 4253–4270. https://doi.org/10.1002/2016WR019767

Voisin, N., Li, H., Ward, D., Huang, M., Wigmosta, M., Leung, L.R., 2013. On an improved sub-regional water resources management representation for integration into earth system models. Hydrol. Earth Syst. Sci. 17, 3605–3622. https://doi.org/10.5194/hess-17-3605-2013

Wada, Y., de Graaf, I.E.M., van Beek, L.P.H., 2016. High-resolution modeling of human and climate impacts on global water resources. J. Adv. Model. Earth Syst. 8, 735–763. https://doi.org/10.1002/2015MS000618

Wang, W., Li, H.-Y., Leung, L.R., Yigzaw, W., Zhao, J., Lu, H., Deng, Z., Demisie, Y., Blöschl, G., 2017. Nonlinear Filtering Effects of Reservoirs on Flood Frequency Curves at the Regional Scale. Water Resour. Res. 53, 8277–8292. https://doi.org/10.1002/2017WR020871

Williamson, C.E., Saros, J.E., Vincent, W.F., Smol, J.P., 2009. Lakes and reservoirs as sentinels, integrators, and regulators of climate change. Limnol. Oceanogr. 54, 2273–2282. https://doi.org/10.4319/lo.2009.54.6_part_2.2273

Wisser, D., Fekete, B.M., Vörösmarty, C.J., Schumann, A.H., 2010. Reconstructing 20th century global hydrography: a contribution to the Global Terrestrial Network-Hydrology (GTN-H). Hydrol. Earth Syst. Sci. 14, 1–24. https://doi.org/10.5194/hess-14-1-2010

Wood, E.F., Roundy, J.K., Troy, T.J., Van Beek, L.P.H., Bierkens, M.F.P., Blyth, E., De Roo, A., Doll, P., Ek, M., Familglietti, J., Gochis, D., Van De Giesen, N., Houser, P., Jaffe, P.R., Kollet, S., Lehner, B., Lettenmaier, D.P., Peters-Lidard, C., Sivapalan, M., Sheffield, J., Wade, A., Whitehead, P., 2011. Hyperresolution global land surface modeling: meeting a grand challenge for monitoring Earth's terrestrial water. Water Resour. Res. 47, 1–10. https://doi.org/10.1029/2010WR010090

Wu, Y., Chen, J., 2012. An Operation-Based Scheme for a Multiyear and Multipurpose Reservoir to Enhance Macroscale Hydrologic Models. J. Hydrometeorol. 13, 270–283. https://doi.org/10.1175/JHM-D-10-05028.1

Wu, Y., Zhang, G., Rousseau, A.N., Jun Xu, Y., Foulon, É., 2020. On how wetlands can provide flood resilience in a large river basin: A case study in Nenjiang River Basin, China. J. Hydrol. 125012. https://doi.org/10.1016/j.jhydrol.2020.125012

Yamazaki, D., de Almeida, G.A.M., Bates, P.D., 2013. Improving computational efficiency in global river models by implementing the local inertial flow equation and a vector-based river network map. Water Resour. Res. 49, 7221–7235. https://doi.org/10.1002/wrcr.20552

Yamazaki, D., Kanae, S., Kim, H., Oki, T., 2011. A physically based description of floodplain inundation dynamics in a global river routing model. Water Resour. Res. 47, 1–21. https://doi.org/10.1029/2010WR009726

Yao, F., Wang, J., Wang, C., Crétaux, J.-F., 2019. Constructing long-term high-frequency time series of global lake and reservoir areas using Landsat imagery. Remote Sens. Environ. 232, 111210. https://doi.org/10.1016/j.rse.2019.111210

Yassin, F., Razavi, S., Elshamy, M., Davison, B., Sapriza-Azuri, G., Wheater, H., 2019. Representation and improved parameterization of reservoir operation in hydrological and land-surface models. Hydrol. Earth Syst. Sci. 23, 3735–3764. https://doi.org/10.5194/hess-23-3735-2019

Yigzaw, W., Li, H.-Y., Demissie, Y., Hejazi, M.I., Leung, L.R., Voisin, N., Payn, R., 2018. A New Global Storage-Area-Depth Dataset for Modeling Reservoirs in Land Surface and Earth System Models. Water Resour. Res. https://doi.org/10.1029/2017WR022040

Yigzaw, W., Li, H.Y., Fang, X., Leung, L.R., Voisin, N., Hejazi, M.I., Demissie, Y., 2019. A Multilayer Reservoir Thermal Stratification Module for Earth System Models. J. Adv. Model. Earth Syst. 11, 3265–3283. https://doi.org/10.1029/2019MS001632

Yoon, Y., Beighley, E., 2015. Simulating streamflow on regulated rivers using characteristic reservoir storage patterns derived from synthetic remote sensing data.

Hydrol. Process. 29, 2014–2026. https://doi.org/10.1002/hyp.10342

Yoon, Y., Beighley, E., Lee, H., Pavelsky, T., Allen, G., 2016. Estimating Flood Discharges in Reservoir-Regulated River Basins by Integrating Synthetic SWOT Satellite Observations and Hydrologic Modeling. J. Hydrol. Eng. 21, 05015030. https://doi.org/10.1061/(ASCE)HE.1943-5584.0001320

You, J.-Y., Cai, X., 2008. Hedging rule for reservoir operations: 1. A theoretical analysis. Water Resour. Res. 44, 1–9. https://doi.org/10.1029/2006WR005481

Zajac, Z., Revilla-Romero, B., Salamon, P., Burek, P., Hirpa, F., Beck, H., 2017. The impact of lake and reservoir parameterization on global streamflow simulation. J. Hydrol. 548, 552–568. https://doi.org/10.1016/j.jhydrol.2017.03.022

Zambon, R., Barros, M.T.L., Yeh, W.W.G., 2018. Evaporation Losses in the Brazilian Hydropower System, in: World Environmental and Water Resources Congress. pp. 85–92.

Zhao, G., Bates, P., Neal, J., 2020. The Impact of Dams on Design Floods in the Conterminous US. Water Resour. Res. 56, 1–15. https://doi.org/10.1029/2019WR025380

Zhao, G., Gao, H., Naz, B.S., Kao, S., Voisin, N., 2016. Advances in Water Resources Integrating a reservoir regulation scheme into a spatially distributed hydrological model R. Elsevier 98, 16–31. https://doi.org/10.1016/j.advwatres.2016.10.014

Zhou, H., Luo, Z., Tangdamrongsub, N., Wang, L., He, L., Xu, C., Li, Q., 2017. Characterizing drought and flood events over the Yangtze River Basin using the HUST-Grace2016 solution and ancillary data. Remote Sens. 9. https://doi.org/10.3390/rs9111100

1493